JCI insight

RESEARCH ARTICLE

Human lung tumor FOXP3+ Tregs upregulate four "Treg-locking" transcription factors

Tatiana Akimova,[1] Tianyi Zhang,[1] Dmitri Negorev,[1] Sunil Singhal,[2] Jason Stadanlick,[2] Abhishek Rao,[2] Michael Annunziata,[2] Matthew H. Levine,[3] Ulf H. Beier,[4] Joshua M. Diamond,[5] Jason D. Christie,[5,6] Steven M. Albelda,[5] Evgeniy B. Eruslanov,[2] and Wayne W. Hancock[1]

[1]Division of Transplant Immunology, Department of Pathology and Laboratory Medicine, and Biesecker Center for Pediatric Liver Diseases, Children's Hospital of Philadelphia and Perelman School of Medicine, University of Pennsylvania, Philadelphia, Pennsylvania, USA. [2]Division of Thoracic Surgery, Department of Surgery, University of Pennsylvania, Philadelphia, Pennsylvania, USA. [3]Department of Surgery, Penn Transplant Institute, Hospital of the University of Pennsylvania and University of Pennsylvania, Philadelphia, Pennsylvania, USA. Department of Surgery, Children's Hospital of Philadelphia, Philadelphia, Pennsylvania, USA. [4]Division of Nephrology, Department of Pediatrics, Children's Hospital of Philadelphia and University of Pennsylvania, Philadelphia, Pennsylvania, USA. [5]Division of Pulmonary, Allergy and Critical Care Medicine, Department of Medicine, and [6]Department of Biostatistics and Epidemiology, University of Pennsylvania, Philadelphia, Pennsylvania, USA.

Experimental data indicate that FOXP3+ Tregs can markedly curtail host antitumor immune responses, but the properties of human intratumoral Tregs are still largely unknown, in part due to significant methodologic problems. We studied the phenotypic, functional, epigenetic, and transcriptional features of Tregs in 92 patients with non–small-cell lung cancer, comparing the features of Tregs within tumors versus corresponding blood, lung, and lymph node samples. Intratumoral Treg numbers and suppressive function were significantly increased compared with all other sites but did not display a distinctive phenotype by flow cytometry. However, by undertaking simultaneous evaluation of mRNA and protein expression at the single-cell level, we demonstrated that tumor Tregs have a phenotype characterized by upregulated expression of FOXP3 mRNA and protein as well as significantly increased expression of EOS, IRF4, SATB1, and GATA1 transcription factor mRNAs. Expression of these "Treg-locking" transcription factors was positively correlated with levels of FOXP3 mRNA, with highest correlations for EOS and SATB1. EOS had an additional, FOXP3 mRNA–independent, positive correlation with FOXP3 protein in tumor Tregs. Our study identifies distinctive features of intratumoral Tregs and suggests that targeting Treg-locking transcription factors, especially EOS, may be of clinical importance for antitumor Treg-based therapy.

Introduction

Lung cancers (LC) are the leading cause of deaths from cancer (1–4). FOXP3+ Tregs are thought to facilitate tumor growth and metastases by inhibition of antitumor immunity (5–8), and accumulation of Tregs within cancers usually corresponds with poor outcomes (4, 6, 9), although exceptions are known (10–12). These inconsistencies suggest that mere enumeration of tumor-infiltrating FOXP3+ cells may not be sufficiently incisive for understanding the biology of Tregs in clinical oncology. Moreover, the origin and properties of intratumoral Tregs in humans remain largely unknown. To address these questions, we explored phenotypic, functional, epigenetic, and transcriptional features of Tregs in a large group of LC patients prior to, and after, operative treatment. We hypothesized that intratumoral Tregs would have a distinctive phenotype, due to upregulation of various Treg-associated markers, providing a basis for Treg-specific targeting in LC patients.

However, studying tumor Tregs is methodologically challenging. Unfortunately, human Tregs cannot be isolated using their FOXP3 expression due to its intranuclear localization, and, as a result, all previous studies necessarily involved Tregs contaminated, at least to some degree, by CD4+FOXP3− conventional T cells (hereafter referred to as Teffs). We overcame this issue using two approaches. First, in functional studies, we used regression analysis to adjust the results of Treg suppression assays according to the FOXP3+

Conflict of interest: The authors have declared that no conflict of interest exists.

Submitted: March 17, 2017
Accepted: July 19, 2017
Published: August 17, 2017

Reference information:
JCI Insight. 2017;2(16):e94075.
https://doi.org/10.1172/jci.insight.94075.

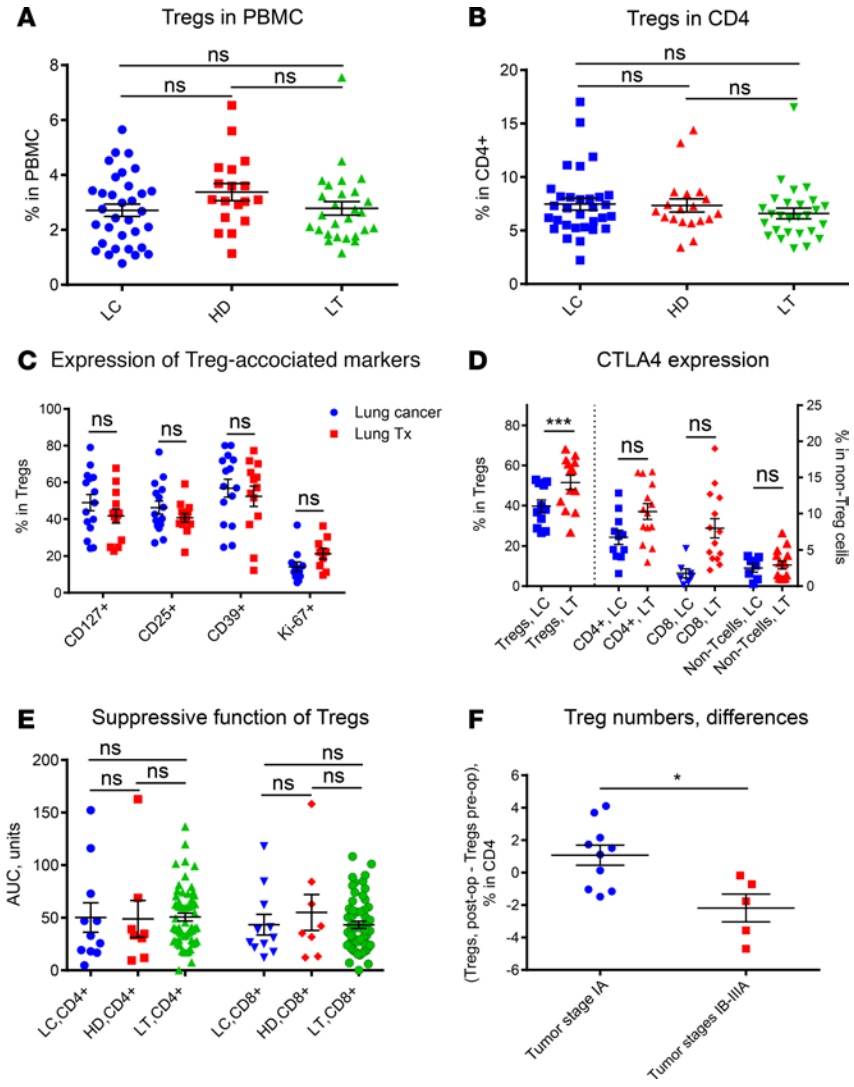

Figure 1. Characteristics of peripheral blood Tregs in LC patients. The frequency of $CD4^+FOXP3^+$ Tregs was evaluated in (**A**) PBMCs and (**B**) $CD4^+$ gated cells by flow cytometry in samples from LC (n = 33), LT (n = 27), and HD (n = 18) groups. Details of the Treg gating strategy are shown in Supplemental Figure 1. Expression of Treg-associated markers was evaluated in (**C**) PBMC Tregs from LC (n = 17) and LT (n = 14) patients, and (**D**) CTLA4 expression was evaluated in all PBMC T cell subsets of the same patients. Gating strategies for each marker are shown in Supplemental Figures 6, 7, 8, and 36. (**E**) $CD4^+CD25^+$ isolated Tregs were incubated with anti-CD3 stimulated CFSE-labeled donor PBMCs in 4-day suppression assay, and Treg-suppressive function was quantified as area under the curve (AUC). 11 LC, 8 HD, and 57 LT patient Treg samples were evaluated. (**F**) LC patients (n = 15) were divided into stage IA and stage IB–IIIA groups, and then percentages of Tregs in $CD4^+$ subsets were compared preoperatively and postoperatively within each patient as the percentage of postoperative Tregs minus the percentage of preoperative Tregs. LC, lung cancer; HD, healthy donors; LT, patients with a lung disease pretransplant; Tx, transplant. The following statistics were used: (**A**, **B**, and **E**) Kruskal-Wallis test; (**C**) multiple t tests with false discovery rate set to 1%; (**D**) ANOVA with post-hoc Holm-Sidak's multiple comparisons test; and (**F**) Mann Whitney test. $^*P < 0.05$; $^{***}P < 0.001$.

purity of isolated Tregs. Second, to analyze the transcriptional features of $FOXP3^+$ Tregs, we applied the PrimeFlow method that allows simultaneous evaluation of mRNA and protein expression at a single-cell level of resolution. Hence, for the first time to our knowledge, mRNA levels were analyzed in pure 100% $FOXP3^+$ Treg populations. We found that lung tumor Tregs have a unique phenotype, with upregulated FOXP3 mRNA and protein and with high expression of 4 of 5 previously reported Treg-locking transcription factors (TFs) (13), namely SATB1, GATA1, EOS, and IRF4, but not LEF1.

Over the years, multiple flow cytometry markers were reported as important for Treg-suppressive function or, to be specific, for Tregs. However, most were characterized using murine cells, with little effort to reevaluate their role in human Tregs, especially in clinical settings. For those that were described in human Tregs, important controls were often missing. Thus, a particular marker cannot be considered as specific for Tregs if it has the same changes in Teffs. Similarly, a cancer-specific marker should be expressed within tumors, but not in tumor-free tissues, whereas blood cells are an inadequate control to assess cancer specificity. We compared expression of 35 commonly used markers in Tregs and Teffs from tumors, tumor-free distant lung tissues, lung lymph nodes (LNs), and blood samples from the same patients and, for each marker, undertook correlation assays to see whether any changes were indeed unique for Tregs or were simply mirrored in Teffs. None of the 35 Treg-associated flow cytometry markers was uniquely expressed by tumor Tregs, despite the increased suppressive function and upregulated expression of Treg-locking TF mRNAs in these cells. Therefore, future therapeutic strategies may require specific attention to this Treg-locking TF quintet as a novel means to decrease Treg function and promote antitumor therapy.

Results

Tregs in the blood of tumor patients are similar to those of control patients. We hypothesized that lung tumors favored Treg development or accumulation and that blood Tregs in LC patients might demonstrate enhanced expression of important Treg-associated markers and/or be more suppressive. Likewise, surgical removal of tumors might reverse these features, with a decrease in Treg numbers and their suppressive function. However, LC patients had no differences in their peripheral blood CD4, CD8, or $CD4^+FOXP3^+$ Treg numbers when compared with healthy donors (HD) or with a reference group consisting of age- and sex-matched patients who were listed for lung transplantation (LT) (Figure 1, A and B; Supplemental Figure 1; and Supplemental Figure 2, A and B; supplemental material available online with this article; https://doi.org/10.1172/jci.insight.94075DS1). LC blood Tregs did not demonstrate any distinctive phenotype based on expression of CD127, CD25, CD39, or Ki67, except for mild downregulation of CTLA4 expression, with similar trends in all other LC Teffs (Figure 1, C and D). The suppressive function of LC blood Tregs, measured by their ability to inhibit the proliferation of activated HD peripheral blood mononuclear cells (PBMCs), did not differ from that of HD or LT patients (Figure 1E). After surgical removal of lung tumors, LC patients did not show any significant change in the number or phenotype of their PBMC Tregs or Teffs (Supplemental Figure 2, C–E). However, when patients were divided according to tumor stage postoperatively, individuals with more advanced stages, IB–IIA, showed decreased numbers of blood Tregs, in contrast to the smallest tumors (Figure 1F). Moreover, patients with the larger tumors had the greatest decreases in Treg numbers (Supplemental Figure 1F). Overall, at early stages, lung tumors appear to have relatively small systemic effects on peripheral blood Treg phenotype, number, or function.

Increased numbers of Tregs in tumors and pulmonary LNs. Even at very early, operable stages of LC, tumors and pulmonary regional LNs were substantially enriched with Tregs (Figure 2, A and B) but not Teffs (Supplemental Figure 3, A and B). Those changes in tumors and LNs appeared to be specific for cancers (Figure 2, B and C). We also observed a cancer-specific decrease in the percentage of $CD8^+$, but not $CD4^+$, cells in pulmonary LNs (Figure 2D and Supplemental Figure 3C), which may reflect ongoing suppression of antitumor cytotoxic T cell immune responses. Several mechanisms have been suggested to explain the Treg enrichment observed in various tumors (14), including their expansion in situ, local inducible Treg (iTreg) conversion, and enhanced trafficking to tumors, and these were explored in our study.

Tregs are not preferentially expanded within lung tumors. Expansion in situ is a straightforward mechanism to explain the increased Treg numbers (15). To assess cellular proliferation, we stained for Ki67, which is expressed during the G_1, S, G_2, and M phases of the cell cycle, whereas G_0 phase cells lack Ki67. Tumor Tregs showed similar Ki67 expression as autologous blood and lung Tregs and were comparable to Tregs from HD (Figure 2E). Moreover, Ki67 expression by Tregs strongly correlated with Ki67 expression by Teffs from the same patient, arguing against preferential tumor-driven division of Tregs versus Teffs (Spearman $r = 0.95$, $P < 0.001$) (Supplemental Figure 3D). Ki67 expression by Tregs was not correlated with the percentage of Tregs in tumors (Supplemental Figure 3E). Moreover, the division of Tregs was negatively correlated with tumor size (Supplemental Figure 3F). Hence, our data do not support increased proliferation as a mechanism to explain increased Tregs within lung tumors.

Tregs do not show increased intratumoral conversion from Teffs. As there are no markers to reliably distinguish iTregs from thymic Tregs (tTregs) (16), we used a composite approach to investigate the frequency of iTregs within tumors. First, we evaluated the expression of two markers that are still widely used as specific determinants of tTregs: Helios and neuropilin. Tumor Tregs had the same levels of those markers as other Tregs (Figure 3, A and B).

Second, we evaluated whether intratumoral conventional cells were prone to convert into iTregs in vitro. Treg-depleted $CD4^+$ Teffs from tumors did not undergo enhanced iTreg conversion when exposed to TCR stimulation, IL-2, and TGF-β (Figure 3C). Finally, as iTregs are typically only partially demethylated within the Treg-specific demethylation region (TSDR) of the FOXP3 locus, in contrast to the completely demethylated TSDR of tTregs (17, 18), we used our recently developed means to assess the ratio of iTreg to tTreg populations (19). This measure is the ratio between FOXP3 protein expression and TSDR demethylation (FOXP3/TSDR) in isolated $CD4^+CD25^+$ Tregs (Supplemental Figure 4A). For the current project, we additionally validated our approach by showing that calcineurin inhibitor (CNI) used in vivo leads to a marked decrease of the FOXP3/TSDR ratio in Tregs (Supplemental Figure 4B), consistent with our pediatric transplant data (19). Healthy male donor Tregs have FOXP3/TSDR ratios of around 1, and this ratio corresponds to 1%–3% of iTregs in peripheral blood, at the limits of sensitivity of the TSDR demethylation

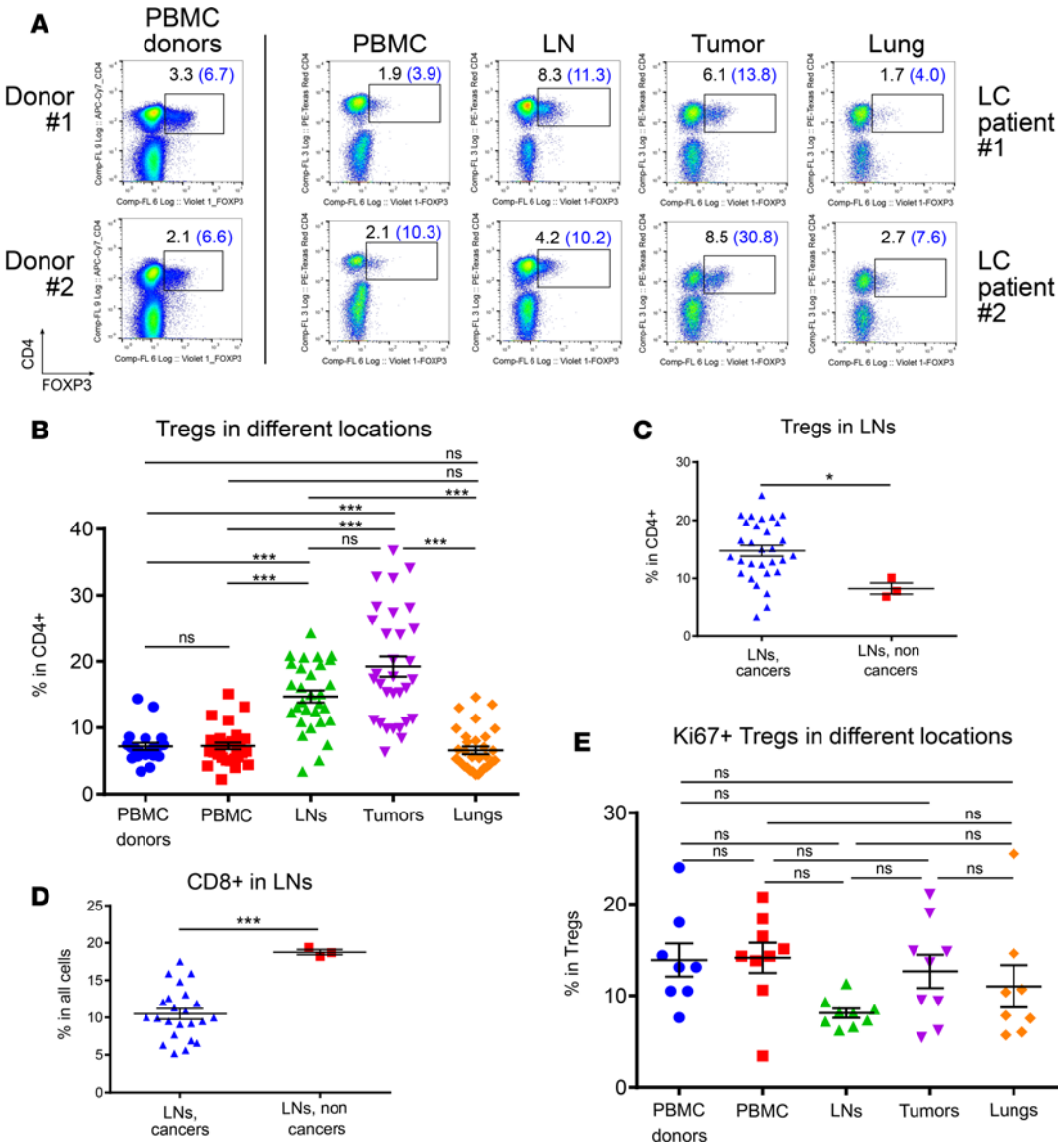

Figure 2. Number and division of intratumoral Tregs. (**A**) The frequency of FOXP3⁺ Tregs was evaluated in all viable cells (indicated) and in CD4⁺ T cells (shown in brackets, blue). Results from two healthy donors, on the left, and two lung cancer patients (on the right) are shown. (**B**) Statistics corresponding to **A**. The frequency of FOXP3⁺ Tregs was evaluated in CD4⁺ T cells in healthy donors (n = 22) and in LC PBMCs (n = 30), LNs (n = 30), tumors (n = 31), and distant lungs (n = 32). Tumor-free distant lung tissues served as controls for tumor-specific versus lung tissue–specific features of Tregs and T cells. The frequencies of (**C**) Tregs in CD4⁺ and (**D**) CD8⁺ cells were compared in lung cancer LNs (n = 30) versus LNs from 3 noncancer patients ("LNs, non cancers," diaphragmatic hernia, sarcoidosis, interstitial lung disease). CD4⁺ subsets in the same LN had no differences (Supplemental Figure 3C). (**E**) Ki-67 expression by CD4⁺FOXP3⁺ Tregs in PBMCs from healthy donors (n = 8), LC PBMCs (n = 8), LNs (n = 9), tumors (n = 9), and distant lungs (n = 8). LNs, lung lymph nodes. The following statistics were used: (**B** and **E**) Kruskal-Wallis test with post-hoc Dunn's multiple comparisons test and (**C** and **D**) Mann Whitney test. *P < 0.05; ***P < 0.001.

assay (Figure 3D). Tumor Tregs did not have any evidence of increased intratumoral iTreg conversion in vivo, as FOXP3/TSDR ratios were the same for tumor, lung, LN, and PBMC Tregs (Figure 3D and Supplemental Figure 4C). However, all Tregs from our LC patients had FOXP3/TSDR ratios of approximately 1.3, which corresponds to approximately 23% of iTregs, which appears to be higher than in HD. Since our LC patients are elderly compared with the HD pool, we questioned if the increased percentage of iTregs might be an age-related phenomenon. To test this hypothesis, we divided the reference group of LT into younger and older patients and compared their FOXP3/TSDR ratios. Indeed, Tregs from older LT patients had elevated FOXP3/TSDR ratios compared with their younger counterparts (Figure 3E). Hence, our data do not support the concept of increased iTreg development within the lung tumors under study but do suggest that age may drive iTreg development.

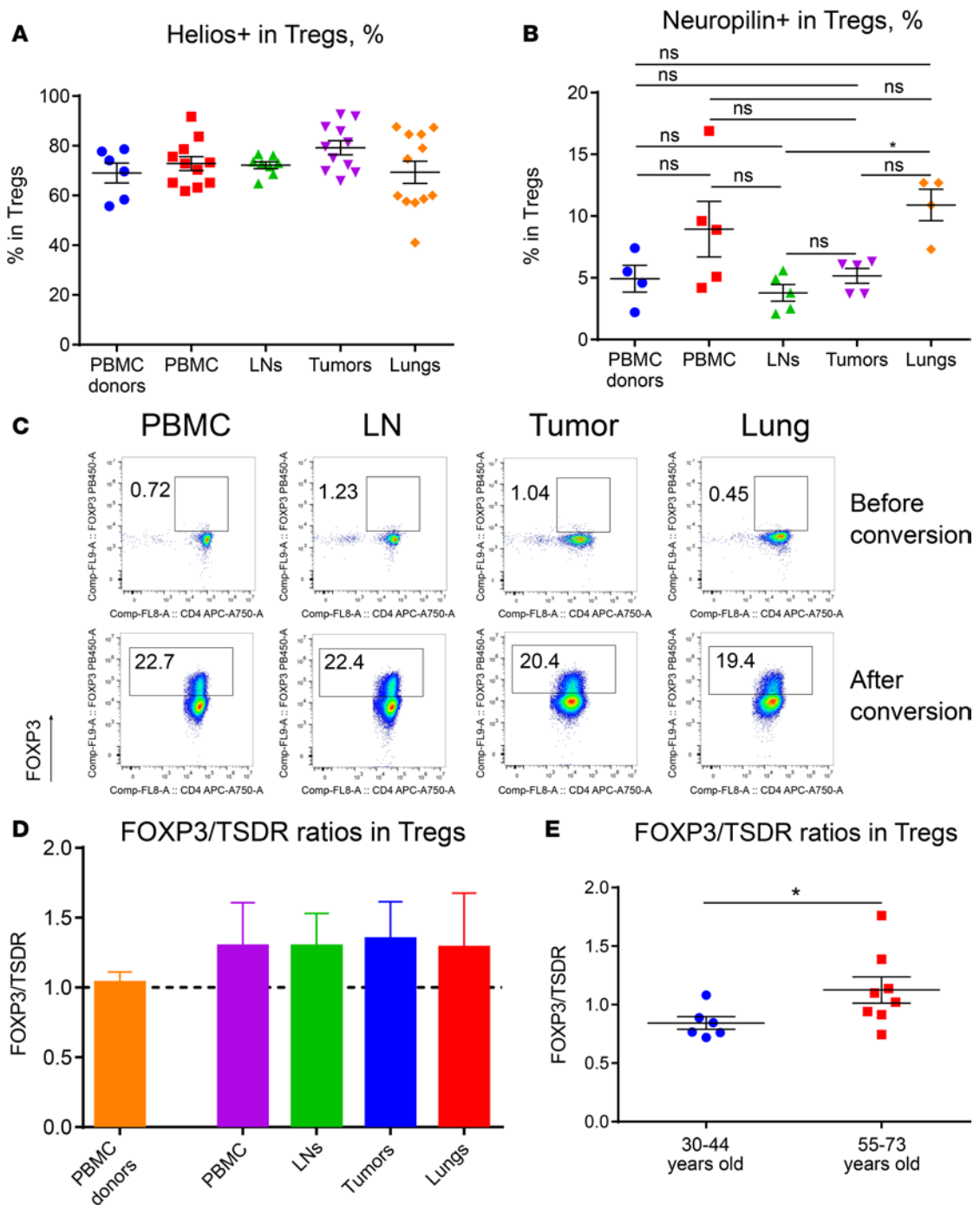

Figure 3. Assessment of intratumoral iTreg conversion. (**A**) Helios and (**B**) neuropilin expression was evaluated in CD4$^+$FOXP3$^+$ Tregs in different samples, including at least 6 (Helios) or 4 (Neuropilin) samples/group; all comparisons for Helios expression were not significant, and the single significant result for Neuropilin is indicated. (**C**) LC PBMCs, LNs, tumors, and distant lung cells were CD25 depleted, and FOXP3$^+$ expression was evaluated in aliquots of starting populations (top row, FOXP3 in CD4$^+$ gated cells). Cells were stimulated with CD3/28 mAbs plus TGF-β and IL-2 for 7 days, and FOXP3$^+$ expression was evaluated as a percentage of in vitro–converted iTregs (bottom row, FOXP3 in CD4$^+$ gated cells); 1 representative experiment of 4 is shown. (**D**) Demethylation of FOXP3 at the TSDR region was evaluated in CD4$^+$CD25$^+$ Tregs. Suppressive function of the same cells was confirmed in suppression assays, and FOXP3$^+$ expression in isolated cells was evaluated by flow cytometry. Ratios between the percentage of FOXP3$^+$ cells and the percentage of TSDR-demethylated cells, FOXP3/TSDR, were counted in all groups: healthy donors (n = 4), LC PBMCs (n = 4), LN (n = 4), tumors (n = 8), and distant lungs (n = 5). To decrease variability, 2–3 technical replicates of TSDR demethylation obtained from the same isolated DNA sample were included, as detailed in Supplemental Figure 4B. (**E**) FOXP3/TSDR ratios were evaluated as described above in Tregs from two groups of LT patients of different ages: the 6 youngest male LT patients, aged 30–44, mean ± SEM 38.5 ± 2.4 years, and 8 males aged 55–73, mean ± SEM 64.9 ± 2.4 years. Gating strategies are shown in Supplemental Figures 1, 12, and 37. The following statistics were used: (**A** and **B**) Kruskal-Wallis test with post-hoc Dunn's multiple comparisons test and (**E**) Mann Whitney test. *P < 0.05.

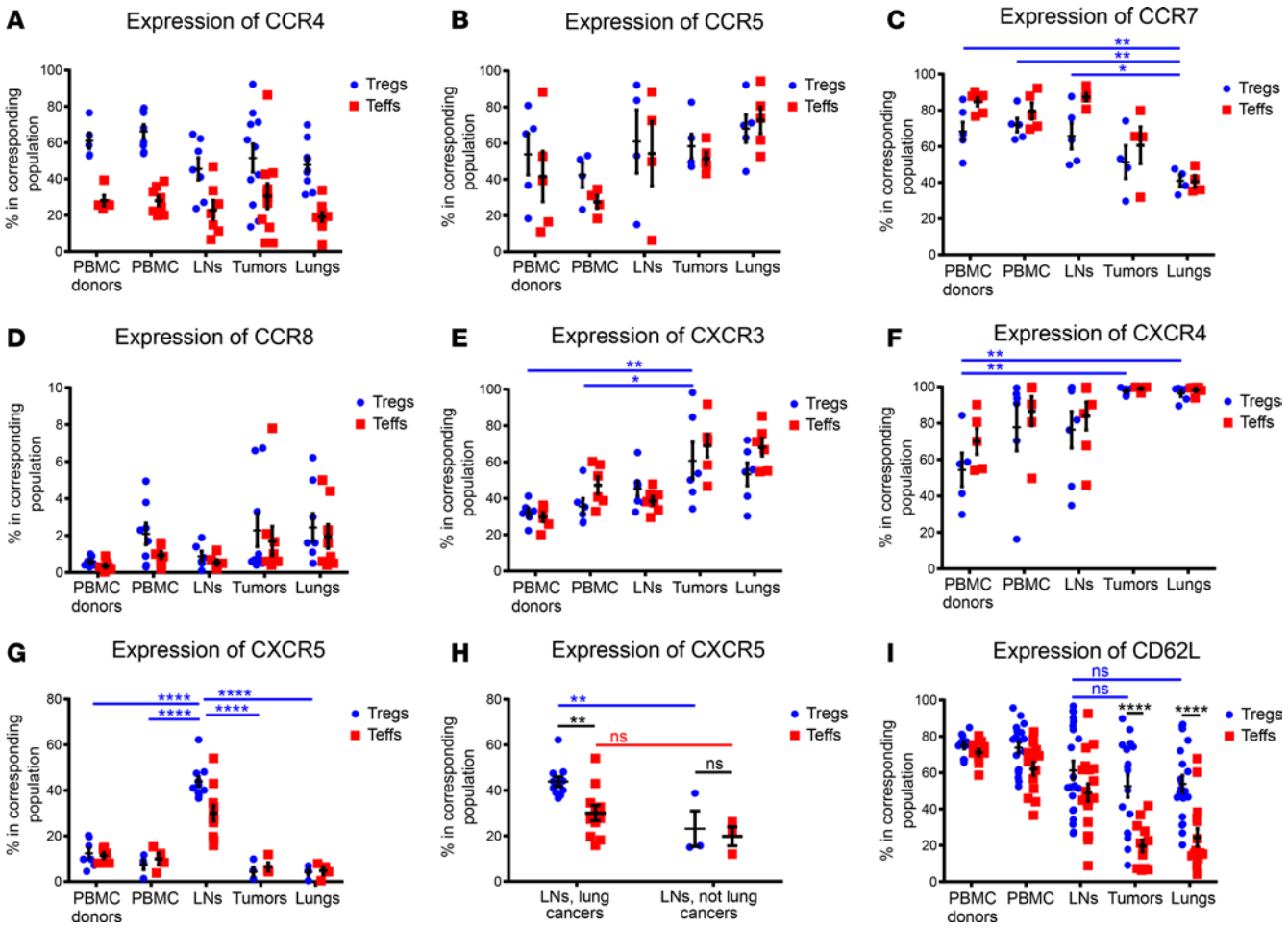

Figure 4. Assessment of intratumoral Treg chemokine receptor expression. (**A**) CCR4, (**B**) CCR5, (**C**) CCR7, (**D**) CCR8, (**E**) CXCR3, (**F**) CXCR4, and (**G**) CXCR5 expression were evaluated in $CD4^+FOXP3^+$ Tregs versus $CD4^+FOXP3^-$ Teffs in different samples, using at least 4 samples/group. (**H**) CXCR5 expression in Tregs versus Teffs were evaluated in lung LNs from patients with adenocarcinoma or squamous cell carcinomas (LNs, lung cancers, $n = 11$) versus LNs from patients with lung metastases of colon cancer or melanoma or with pulmonary sarcoidosis ($n = 3$, LNs, not lung cancers). (**I**) Expression of CD62L was evaluated in Tregs versus Teffs in different samples, using at least 11 samples/group. The following statistics were used: 2-way ANOVA with Tukey's multiple comparisons test for row factor, a location of either Tregs or Teffs (PBMCs versus LNs versus tumors etc.), and with Sidak's multiple comparisons test for column factor to compare expression in Tregs versus Teffs. $^*P < 0.05$; $^{**}P < 0.01$; $^{****}P < 0.0001$. For **A–G**, only significant values in row factor in Tregs are shown in figures, full data are presented in Supplemental Tables 8 and 9. Blue lines indicate comparisons between Tregs, red lines indicate comparisons between Teffs, and black lines indicate comparisons between Tregs and Teffs.

Tregs in LNs of LC patients have increased CXCR5 expression. Preferential Treg trafficking to tumors is a third potential mechanism responsible for their accumulation within tumors, and this mechanism may provide an important tool to regulate antitumor immunity. We examined the expression of several previously reported tumor-relevant chemokine/cytokine receptors in our samples from different locations and found no statistically significant differences in expression of CCR4, CCR5, CCR7, CCR8, CXCR3, or CXCR4 (Figure 4, A–G). Although we observed a higher percentage of expression of CCR4 in Tregs versus Teffs in tumors, these differences were not cancer specific, because Tregs had more CCR4 in multiple other anatomic locations, and the same Treg-Teff differences were observed in HD. However, we found a marked increase in CXCR5 expression by $CD4^+$ T cells within LNs of LC patients, and expression was significantly higher in Tregs than in Teffs (Figure 4G). This Treg-specific upregulation of CXCR5 in lung LNs was observed only in LC patients, whereas LNs from patients with lung metastases from colon cancer or melanoma, and LNs from a patient with sarcoidosis, had significantly less CXCR5 expression and no differences between Tregs and Teffs (Figure 4H). Unfortunately, the design of the current study did not support collection of more noncancer pulmonary LNs to further study CXCR5 expression.

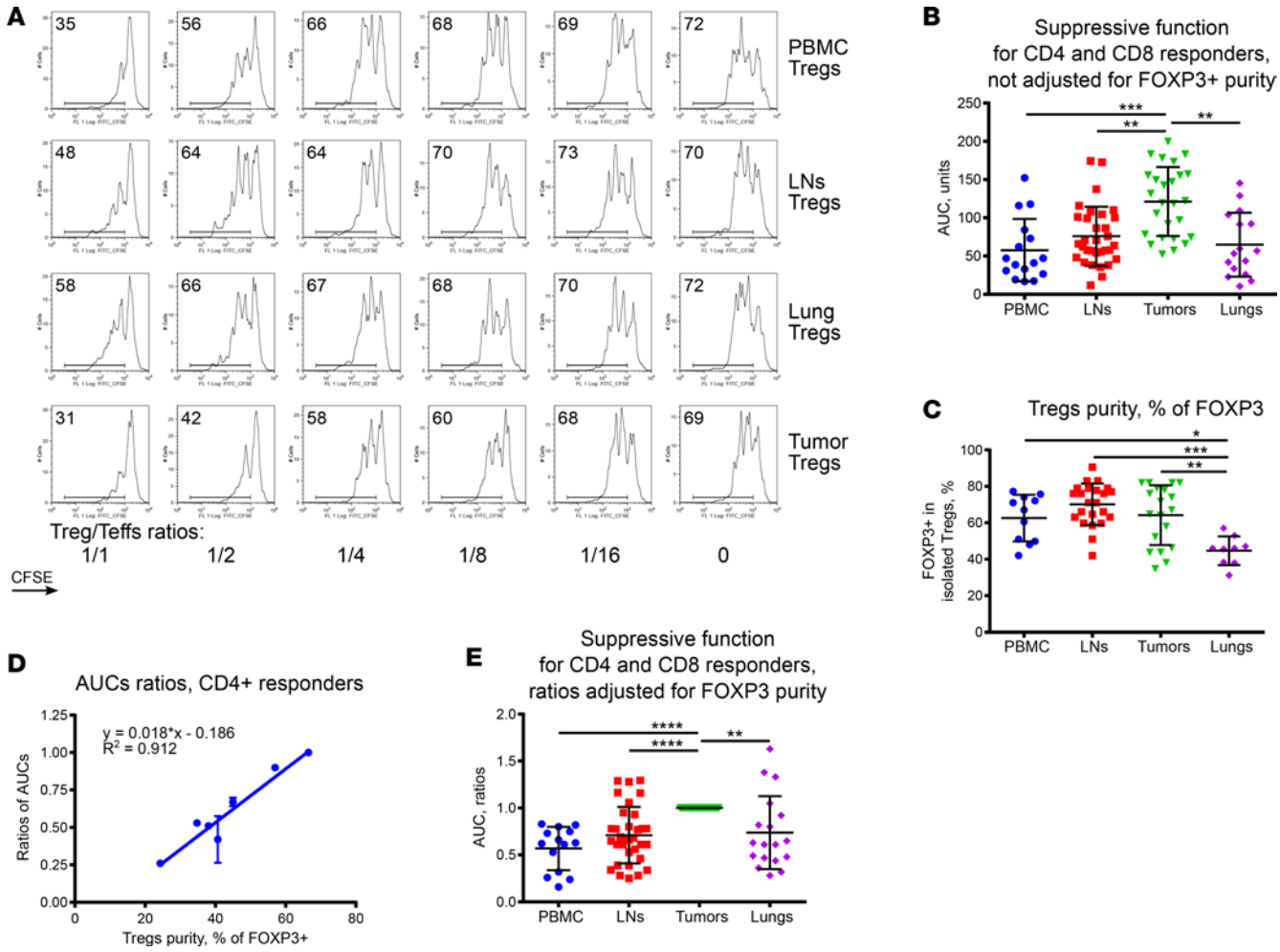

Figure 5. Suppressive function of Tregs. (**A**) Treg-suppressive function using CFSE$^+$CD4$^+$ healthy donor responders; 1 representative experiment of 45 is shown. (**B**) Treg-suppressive function from **A** was calculated in AUC units, as described in Methods. (**C**) FOXP3$^+$ expression in aliquots of all isolated Tregs presented in **B**. (**D**) Resulting equation of regression analysis performed with 5 Treg samples with different FOXP3$^+$ purities, as described in Results. (**E**) Treg-suppressive function presented in **B** and **C** was recalculated according to **D** to adjust for different Treg FOXP3$^+$ purity. Then tumor Treg function was set up as 1, and suppressive functions of Tregs, isolated from different locations in the same patient, were compared with tumor Tregs. Final results include technical replicates of some experiments (total n = 52). The following statistics were used: (**B**) Kruskal-Wallis test with post-hoc Dunn's multiple comparisons test; (**C**) ANOVA with Tukey's multiple comparisons test; (**D**) linear regression analysis; and (**E**) 1-sample t test with mean = 1. $^*P < 0.05$; $^{**}P < 0.01$; $^{***}P < 0.001$; $^{****}P < 0.0001$.

As cells may downregulate their chemokine receptors when they reach the target tissue, we studied whether CXCL13, a ligand for CXCR5, was upregulated in lung tumors, but found no mRNA upregulation in comparison with LC LN or distant lung tissues (Supplemental Figure 4D). Lung tumor and distant lung Tregs also expressed CD62L at levels comparable with LN Tregs, in contrast to the majority of lung tissue and tumor Teffs that lack CD62L expression (Figure 4I). The relatively high CD62L expression in Tregs was not related to an increased number of naive Tregs versus Teffs, as both T cell subsets had similarly downregulated CD45RA and upregulated CD45RO expression in lung tissues and tumors (Supplemental Figure 4, E and F), and there are fewer naive Tregs than Teffs in all locations. Taken together, the relatively high CD62L expression in lung and tumor Tregs, as compared with Teffs, suggests enhanced trafficking of Tregs between tumors and lung LNs, but the LC-specific increase of CXCR5$^+$ Tregs in pulmonary LNs, in the absence of upregulated expression of its ligand CXCL13 in tumors, may be due to the increased number of follicular Tregs (20, 21) in LC LN, rather than due to differential Treg tumor trafficking.

Tumor Tregs have enhanced suppressive function. There are very few reports of the functional characterization of Tregs isolated from clinical tumors. To avoid confounding variables due to differences in patient Teffs and antigen-presenting cells (such as differences in resistance to suppression, cell viability or

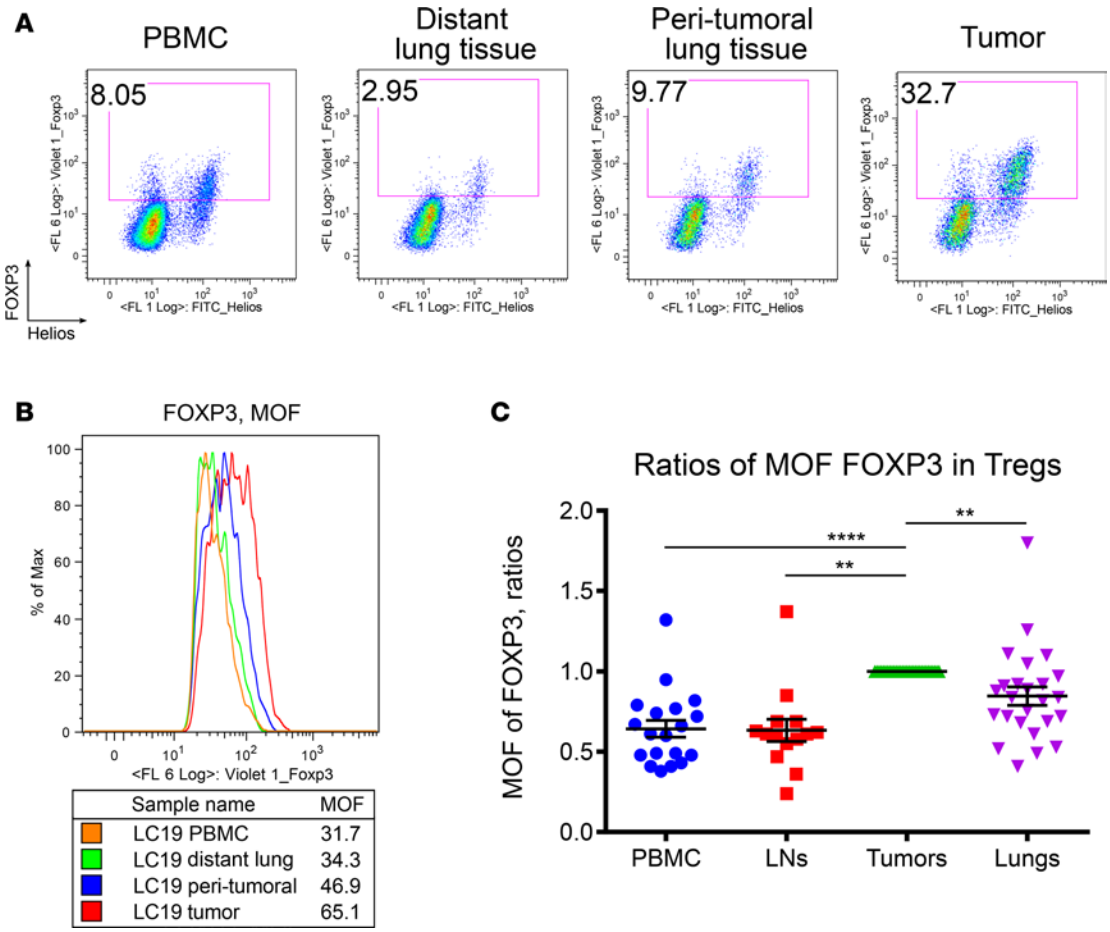

Figure 6. Tumor Tregs have more FOXP3 protein than other Tregs. (**A**) Representative staining of FOXP3$^+$ Tregs from different locations in the same patient and (**B**) corresponding histograms showing median of fluorescence (MOF) for FOXP3 protein/cell in CD4$^+$FOXP3$^+$ gated cells. (**C**) Evaluation of FOXP3 MOF in CD4$^+$FOXP3$^+$ Tregs of 89 samples, including at least 14 samples/group, with tumor Treg FOXP3 MOF in each experiment set as 1. The following statistics were used: (**C**) Wilcoxon signed-rank test with median = 1. $^{**}P < 0.01$; $^{****}P < 0.0001$.

costimulatory capacities), we used a highly standardized suppression assay (22). Aliquots of the same cryopreserved sample of HD PBMCs were used as responder cells for all studies, and only patient Tregs differed between experiments. Tumor Tregs demonstrated powerful suppression of proliferation of responder CD4 and CD8 T cells, which was significantly increased in comparison to Tregs from any other anatomic location (Figure 5, A and B, and Supplemental Figure 5A).

To ensure that the observed differences in functional activity were caused by increased Treg-suppressive ability and not due to differences in the FOXP3 purity of CD4$^+$CD25$^+$ Tregs, we evaluated all isolated Tregs for their FOXP3 expression. Although PBMC, LN, and tumor Tregs had comparable purity of cells in functional tests, the isolation of Tregs from lungs in every experiment was associated with decreased FOXP3$^+$ purity (Figure 5C). However, distant lung Tregs are a key control for tumor Tregs, so that we can distinguish differences due to their location in peripheral tissue versus a cancer-specific change. To overcome the problem of having differences in Foxp3$^+$ purity after cell isolation, we established a standard curve accounting for Foxp3$^+$ Treg purity: that is, we assembled Tregs from 3 LC patients and 2 HD, in which the isolated Tregs were diluted with autologous FOXP3$^-$CD4$^+$CD25$^-$ Teffs so we could precisely compare the suppressive function of Tregs at known different purities ranging from 40% to 100%. We then quantified how a reduction in Foxp3$^+$ Treg purity decreased Treg-suppressive function (Figure 5D, Supplemental Figure 5B, and Supplemental Table 1). The resultant equations of regression analyses (Supplemental Table 2) were subsequently used to predict suppressive function of two control independent Treg samples, one from a HD and one from a LC patient (distant lung Tregs). Prediction errors ranged between 1% and 10% (CD4 and CD8 responders) at 48% FOXP3$^+$ purity and between 15% and 18% for 22% FOXP3$^+$ purity (Supplemental Figure 5, C and D,

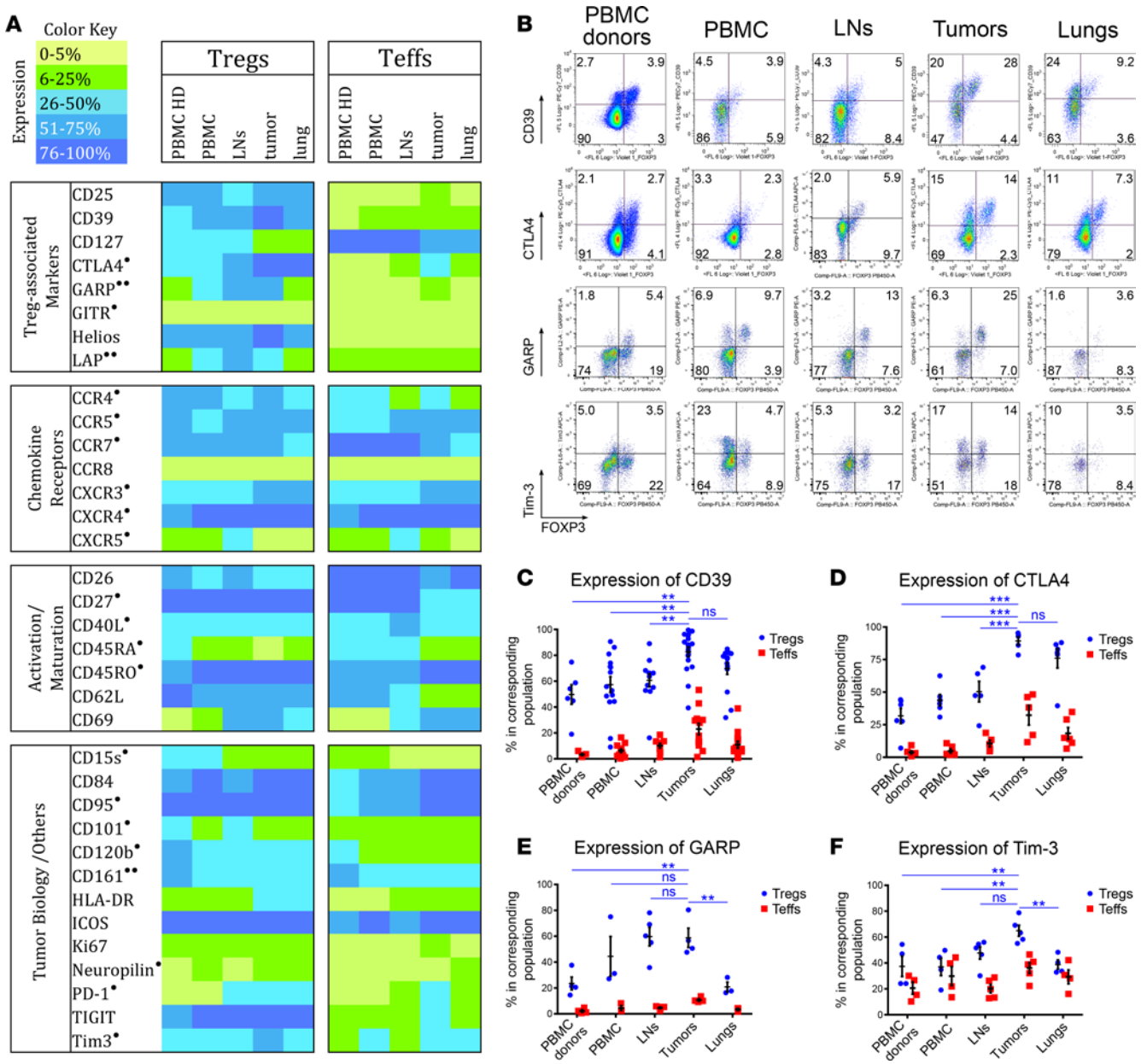

Figure 7. Phenotype of Tregs in different anatomic locations. (**A**) Heatmap indicating expression of 35 markers that were evaluated in CD4$^+$FOXP3$^+$ Tregs versus CD4$^+$FOXP3$^-$ Teffs in different samples. In total, we evaluated markers in 1,295 Treg-Teff pairs in 301 lung cancer samples, and each marker was evaluated at least 4 (for nonstimulated cells) or 3 (for GARP and LAP) times in different samples. All multiple technical replicates were omitted from the final count leaving only 1 value per 1 unique sample. •, data representative for adenocarcinoma and squamous cell carcinoma patients; ••, only adenocarcinoma patient and healthy donor data; no marks, all types of cancers data shown, with no apparent differences between cancer types. (**B**) Representative plots and (**C**–**F**) final statistics for the best tumor Treg-specific candidate markers. The following statistics were used: (**A**) mean of expression in each group and (**C**–**F**) 2-way ANOVA with Tukey's multiple comparisons test for row factor, a location of either Tregs or Teffs (PBMC vs. LNs vs. tumors etc.), and with Sidak's multiple comparisons test for column factor, to compare expression in Tregs versus Teffs. $^{**}P < 0.01$; $^{***}P < 0.001$. Only statistics in row factor in tumor Tregs are shown, full data are shown in Supplemental Table 5. Gating strategies for each marker are shown in Supplemental Figures 6–40.

and Supplemental Table 3). After adjustment of Treg-suppressive function for Treg FOXP3$^+$ isolation purity, tumor Tregs were confirmed to be the most powerful suppressors, with almost twice as much suppressive function as peripheral blood Tregs (Figure 5E).

Tumor Tregs have significantly more FOXP3 protein per cell but no unique phenotypic markers. We next assessed whether the significantly enhanced suppressive functions of tumor Tregs were associated with any distinctive phenotypic features. Tumor Tregs had more FOXP3 protein per cell, and the FOXP3 protein level gradually decreased in tumors comparing those from peritumoral areas to those from the most distant

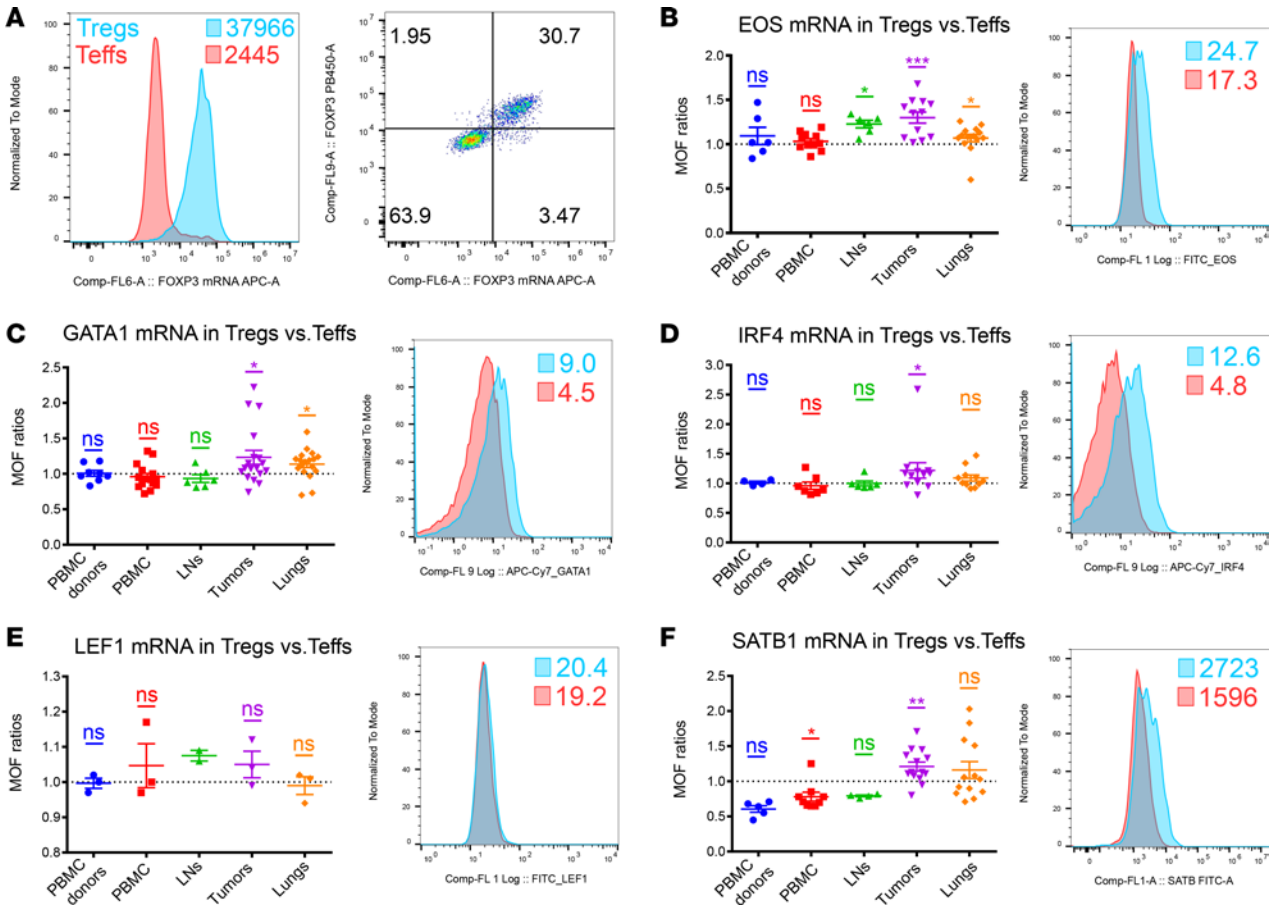

Figure 8. Expression of mRNAs of FOXP3 and the quintet of Treg-locking TFs in Tregs versus Teffs. mRNA expression of (**A**) FOXP3, (**B**) EOS, (**C**) GATA1, (**D**) IRF4, (**E**) LEF1, and (**F**) SATB1 were evaluated in $CD4^+FOXP3^+$ gated Tregs versus $CD4^+FOXP3^-$ Teffs using PrimeFlow method. (**A**) Representative histogram of FOXP3 mRNA expression in tumor Tregs (blue) versus Teffs (red), with corresponding MOF is shown on the left, while the FOXP3 mAb (*y*) versus FOXP3 mRNA (*x*) plot on the right shows a representative example of one tumor $CD4^+$ gated sample. (**B–F**) MOF of each TF in Tregs was set as 1 to compare with MOF in corresponding Teffs, and resulting statistics are shown on the left. Histograms on the right show representative expression, with MOF in tumor Tregs (blue) and Teffs (red). In total, mRNA levels were compared in 213 Treg-Teff pairs, with at least 3 samples (LEF1 only) or at least 4 samples (other TFs) in each group. The following statistics were used: (**B–F**) Wilcoxon signed-rank test with median = 1. $*P < 0.05$; $**P < 0.01$; $***P < 0.001$.

adjacent lungs (Figure 6). In a search for additional phenotypic characteristics, we tested expression of 35 flow cytometry markers, using 262 samples (PBMCs, lungs, LNs, tumors) from 71 LC patients and 23 HD, and evaluated 1,279 pairs from Treg and Teff populations in total (Figure 7A and Supplemental Figures 6–40). The tested markers have previously been suggested to be important for Treg function, to be upregulated in tumor Tregs and/or related with tumor T cells and Treg biology, to serve as selective Treg-positive or Treg-negative markers, or to be important for tumor Treg or Teff trafficking (Supplemental Table 4).

An ideal tumor Treg marker would (a) be differentially expressed by Tregs versus Teffs, i.e., Treg specific; (b) be significantly upregulated in tumor versus other Tregs, i.e., tumor specific; and (c) correlate with Treg-suppressive function. Most Treg-associated markers suggested to be related to Treg function or to be selective for Tregs passed the first requirement and were differentially expressed by Tregs versus Teffs: CD25, CD39, CTLA4, GARP, GITR, Helios, LAP, Tim3, and TIGIT were upregulated, while CD127 and CD26 were downregulated (Figure 7A). Additionally, we found higher expression of CD15s, CD95, and CD120b in Tregs versus Teffs, but only in PBMCs and LNs (Figure 7A and Supplemental Figures 28, 30, and 32). With regard to the second requirement, we identified 4 promising candidates: CD39, CTLA4, GARP, and Tim3 (Figure 7, B–F, and Supplemental Table 5). Tumor Tregs highly expressed all 4 markers, with Tim3 showing the highest difference, but none reached significance for tumor Treg expression versus all other anatomic locations. Thus, CD39 and CTLA4 were similarly upregulated in Tregs in tumors but were also increased in nontumor distant lung samples, while GARP expression was

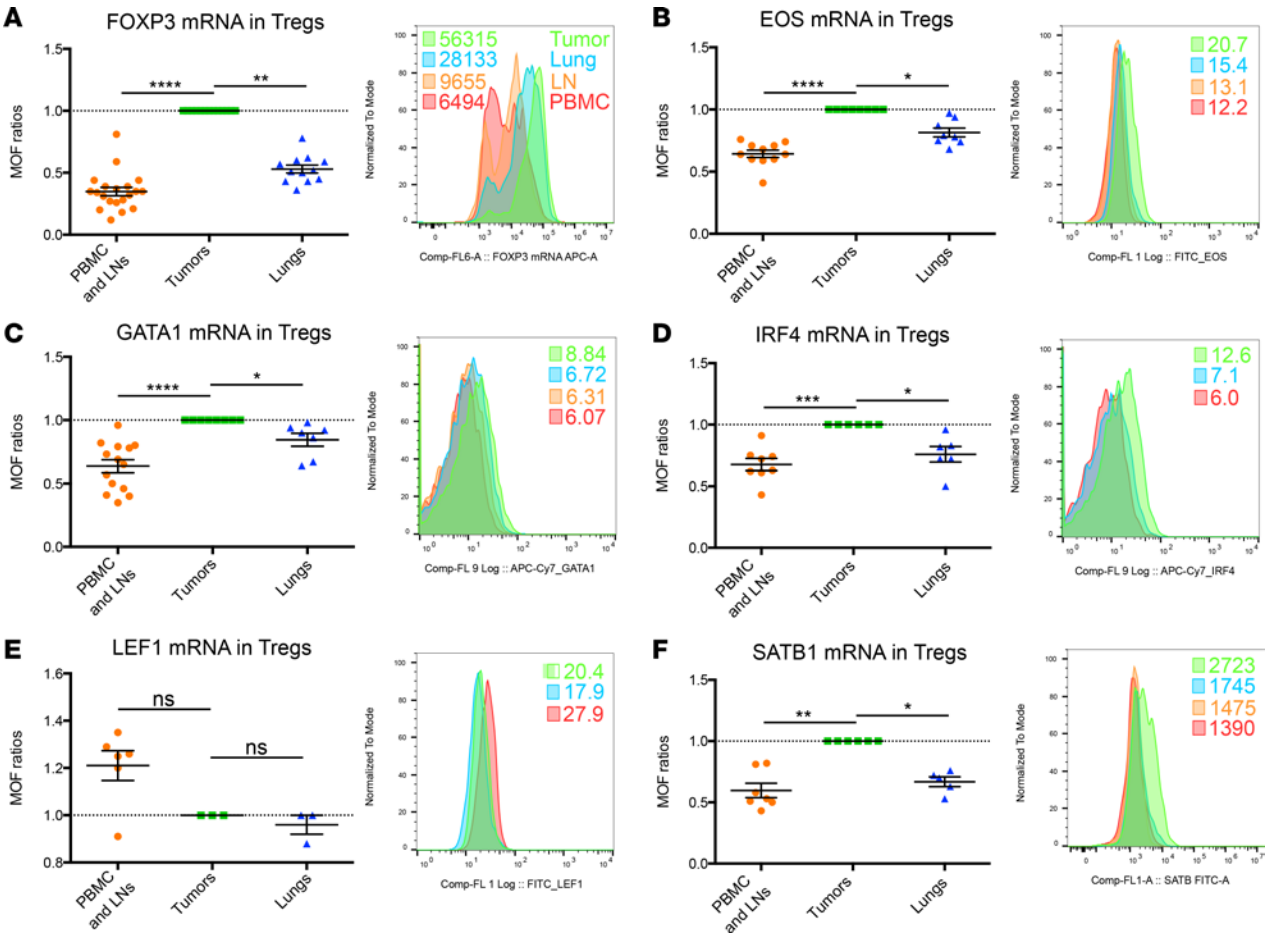

Figure 9. Expression of mRNAs of FOXP3 and the quintet of Treg-locking TFs in tumor versus other Tregs. mRNA expression of (**A**) FOXP3, (**B**) EOS, (**C**) GATA1, (**D**) IRF4, (**E**) LEF1, and (**F**) SATB1 were evaluated in CD4$^+$FOXP3$^+$ gated Tregs from PBMCs, LNs, tumors, and distant lungs using the PrimeFlow assay. MOF of each TF in tumor Tregs was set as 1 to compare with MOF in other Tregs evaluated in the same experiment. Resulting statistics are shown on the left. Histograms on the right show the representative expression, with MOF in PBMCs (red), LNs (orange), and distant lung (blue) and tumor (green) Tregs. mRNAs were compared at least in 3 samples (LEF1 only) or at least in 5 samples (other TFs) per indicated group for each TF, with 28 unique samples and 135 comparisons. The following statistics were used: Kruskal-Wallis test with post-hoc Dunn's multiple comparisons test. *$P < 0.05$; **$P < 0.01$; ***$P < 0.001$; ****$P < 0.0001$.

increased to the same extent in Tregs of tumors and LNs. Moreover, expression of the best candidates, and almost all of the other markers, was closely correlated between Tregs and Teffs (Supplemental Figures 6–40), suggesting a shared mechanism of regulation, and, therefore, an absence of any unique tumor Treg signature. The exceptions, markers which did not demonstrate significant correlation of their expression in Tregs versus Teffs, were CD25, LAP, CD15s, CD95, CD120b, and TIGIT (Supplemental Figures 6, 13, 28, 30, 32, and 39). Due to the absence of a unique tumor Treg candidate marker, we did not test correlations with Treg-suppressive function. In summary, despite an exhaustive analysis, beyond expression of FOXP3 protein itself, none of the 35 flow cytometric markers widely used to study Tregs was able to define a tumor-specific Treg population.

Tumor Tregs upregulate FOXP3 mRNA and a set of "Treg-locking phenotype" TFs. Given an absence of specific membrane markers, human Tregs cannot be isolated for standard qPCR with high purity, an issue that is even more complicated for lung tissue samples (Figure 5C). To resolve this problem, we applied the PrimeFlow method, which allows simultaneous measurement of mRNA and protein by flow cytometry (23) (Figure 8A and Supplemental Figure 41). By gating on FOXP3$^+$ cells, we were able to evaluate mRNA expression of target genes in human Tregs that were 100% pure. While FOXP3 mRNA expression was indeed specific for FOXP3 mAb–gated Tregs (Figure 8A), the expression of housekeeping gene mRNA, as well as that of unrelated genes, did not differ between Tregs and Teffs (Supplemental Figure 42A and Supplemental Figure 43 as well as Supplemental Tables 10 and 11), attesting to the specificity of this method.

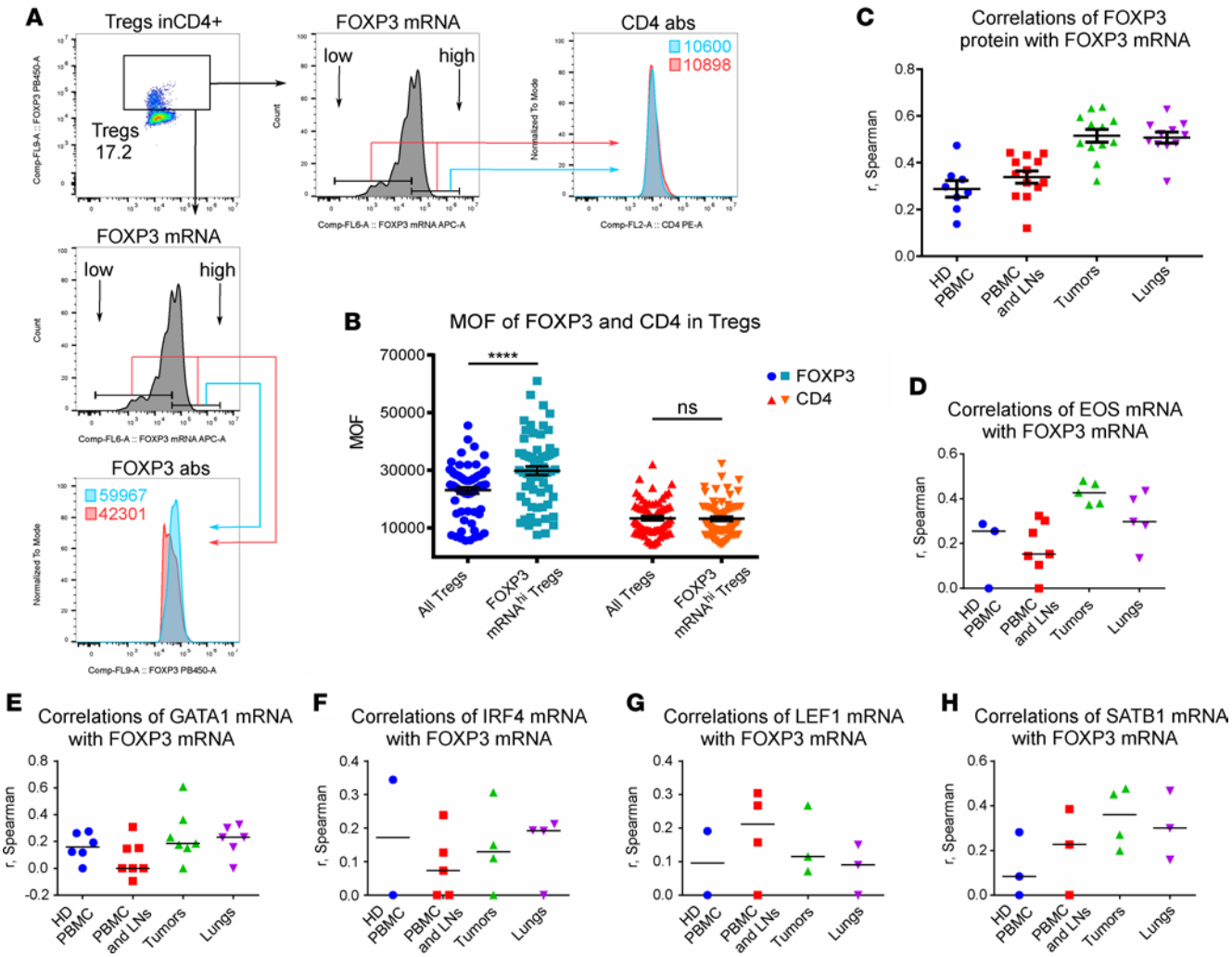

Figure 10. Correlations of Treg-locking TF expression and FOXP3 mRNA in Tregs. (**A**) CD4$^+$FOXP3$^+$ gated Tregs were divided into two populations according to their levels of FOXP3 mRNA expression: top 50% ("high") and bottom 50% ("low"), as shown. Then MOF of FOXP3 protein (left, bottom) and MOF of CD4 protein (right, top) were evaluated in FOXP3 mRNA "high" (blue) versus all Tregs (red) populations. Histograms show MOF in one representative tumor sample, and (**B**) statistics are shown for 64 samples in each group. Tregs from all locations were evaluated together. (**C–H**) Data of fluorescence for markers of interest in CD4$^+$FOXP3$^+$ gated Tregs were collected using PrimeFlow method, exported as data for all channels in each individual Treg, log10 transformed, and evaluated for correlations between (**C**) FOXP3 protein and FOXP3 mRNA expression, (**D**) EOS mRNA and FOXP3 mRNA, (**E**) GATA1 mRNA and FOXP3 mRNA, (**F**) IRF4 mRNA and FOXP3 mRNA, (**G**) LEF1 mRNA and FOXP3 mRNA, and (**H**) SATB1 mRNA AND FOXP3 mRNA. 1,000 Tregs (mean ± SEM) were evaluated in each sample, and each TF was evaluated at least twice (for healthy donors only) or 3 times, in different samples. The following statistics were used: (**B**) Friedman test with Dunn's test; (**D–H**) Spearman correlation assays, correlation coefficients *r* are presented. ****$P < 0.0001$. When *P* values for Spearman correlation were >0.05, then *r* values are shown as zeroes.

A recently described "Treg-locking quintet" of TFs was postulated to promote a Treg-specific gene signature and to enhance occupancy by FOXP3 at its genomic targets when FOXP3 mRNA and any 1 of 5 TFs are expressed (13). When we compared mRNA expression of the TF quintet in Tregs versus Teffs, we found that TF expression varied in different cell subsets (Figure 8, B–F). Thus, Tregs from peripheral blood and LNs have downregulated SATB1, whereas tumor Tregs significantly upregulated SATB1 in comparison with Teffs. Only tumor Tregs reproducibly upregulated 4 of the 5 TFs, SATB1, IRF4, EOS, and GATA1, to levels significantly higher than in corresponding Teffs (Figure 8, B–F).

To study whether expression of Treg-locking TFs is increased in tumor versus nontumor Tregs, we applied PrimeFlow to tumor, lung, LN, and blood samples. We found the same 4 TFs, SATB1, IRF4, EOS, and GATA1, were significantly upregulated in tumor Tregs (Figure 9) and that tumor Tregs, but not Tregs from other anatomic locations, produced large amounts of FOXP3 mRNA (Figure 9A and Supplemental Figure 42B). Only these 4 TFs, and not mRNAs of housekeeping or nonrelated genes, were upregulated in

tumor Tregs versus other Tregs (Supplemental Figure 42C). Therefore, expression of 4 TFs, SATB1, IRF4, EOS, and GATA1, in tumor Tregs completely satisfied the criteria for tumor Treg–specific markers in that they were both Treg and tumor specific.

Single-cell analysis of FOXP3 mRNA versus protein in Tregs. To study how upregulation of Treg-locking TFs is related with the expression of FOXP3, the key Treg lineage master regulator, and to compare the strength of effects between different TFs, we performed single-cell analyses of FOXP3 mRNA, FOXP3 protein, and Treg-locking TF mRNA expression in Tregs. We found that Tregs with upregulated FOXP3 mRNA, i.e., gated cells with a greater than median level of FOXP3 mRNA expression, had significantly more FOXP3 protein per cell (Figure 10, A and B). This suggests that tumor Tregs do not have increased FOXP3 mRNA levels to compensate for its loss due to FOXP3 protein instability, but rather upregulate FOXP3 protein levels above usual levels through active synthesis. We then analyzed the correlations between FOXP3 mRNA and FOXP3 protein expression in Tregs from different locations. Methodologically, we evaluated the fluorescent intensity data for FOXP3 mRNA and FOXP3 protein channels on the single-cell levels in 1,000 $CD4^+FOXP3^+$ Tregs from each sample. Tumor and lung tissue Tregs demonstrated the highest FOXP3 mRNA-to-protein correlation, while peripheral Tregs in blood and LNs had the same correlation coefficients as HD blood Tregs (Figure 10C). Notably, all Treg-locking TFs, including LEF1, demonstrated positive correlations between their mRNA levels and FOXP3 mRNA expression in Tregs at the single-cell level (Figure 10, D–H), confirming initial observations using transduced murine Teffs (13). Within all TFs, EOS and SATB1 showed the highest correlation coefficients, especially in tumor Tregs (Figure 10, D and H).

Single-cell data also showed that mRNA expression of most TFs correlated with FOXP3 protein expression in cancer Tregs, suggesting that those TFs may positively regulate FOXP3 protein at the posttranscriptional level. However, given the previously noted correlations between the TF quintet with FOXP3 mRNA and FOXP3 mRNA with FOXP3 protein, the correlations between TF mRNA and FOXP3 protein might be secondary to the other two observations. To assess if the correlation between TFs and FOXP3 protein was an independent finding, we evaluated partial correlations between TFs and FOXP3 protein, while controlling for the effect of FOXP3 mRNA (Figure 11). Partial correlation analysis showed that only EOS had an additional effect on regulation of FOXP3 at the posttranscriptional level, and this effect was evident only in tumor and lung Tregs (Figure 11E and Supplemental Table 6). Therefore, tumor Tregs have a unique phenotype with largely upregulated FOXP3 protein and FOXP3 mRNA expression, and all Treg-locking TFs positively regulate FOXP3 mRNA. In addition, EOS mRNA demonstrated the highest correlation with FOXP3 mRNA, and EOS is likely involved in the posttranscriptional regulation of FOXP3.

The phenotype of tumor Tregs is unstable and may be governed by the tumor microenvironment. We studied whether the tumor Treg phenotype was stable when the cells were removed from the tumor environment and whether nontumor Tregs can increase expression of FOXP3 protein, FOXP3 mRNA, and Treg-locking TF mRNAs. FOXP3 protein expression per cell decreased in tumor Tregs incubated in vitro as single-cell suspensions. However, tumor-derived soluble factors tended to rescue levels of FOXP3 when 50% of cell media was replaced by tumor-conditioned media (TCM) (Figure 12A). Tumor Tregs also decreased their FOXP3 mRNA expression, while peripheral Tregs incubated with TCM or distant lung-conditioned media (NCM) tended to upregulate their FOXP3 mRNA and, in some experiments, reached levels comparable with those of ex vivo tumor Tregs (Figure 12B). We also observed that expression of GATA1, EOS, IRF4, and SATB1 mRNAs slightly decreased in tumor Tregs in vitro, with no apparent changes in PBMC, LN and lung Tregs (Figure 12, C–F). On average, tumor Tregs expressed 13% less TF mRNA after in vitro incubation. In contrast, peripheral Tregs tended to increase mRNA of Treg-locking TFs when incubated with TCM (Figure 12C). Therefore, the phenotype of tumor Tregs is not stable, and tumor-derived soluble factors are not sufficient to induce similar tumor Treg features as observed in the tumor microenvironment, yet these TCM factors promote upregulation of FOXP3 mRNA in peripheral Tregs. Interestingly, in tumor Tregs, we observed dissociation between FOXP3 mRNA and protein levels in cells incubated in TCM; while Tregs lost about 40% of mRNA, they lost less than 10% of FOXP3 protein (Figure 12, A and B). Such data suggest that soluble factors from the tumor microenvironment are present in TCM and may be able to positively regulate stability of FOXP3 protein in tumor Tregs in complex ways, i.e., regulate FOXP3 at the posttranslational level.

Candidate regulatory factors in the tumor microenvironment. To study what factors in TCM might drive upregulation of FOXP3 mRNA, we performed qPCR of patient PBMC, LN, tumor, and lung samples using a set of the most promising candidates, based on expression in the lung tumor microenvironment and/or their importance in Treg biology. We analyzed expression of TGF-β (24, 25), IL-10 (7),

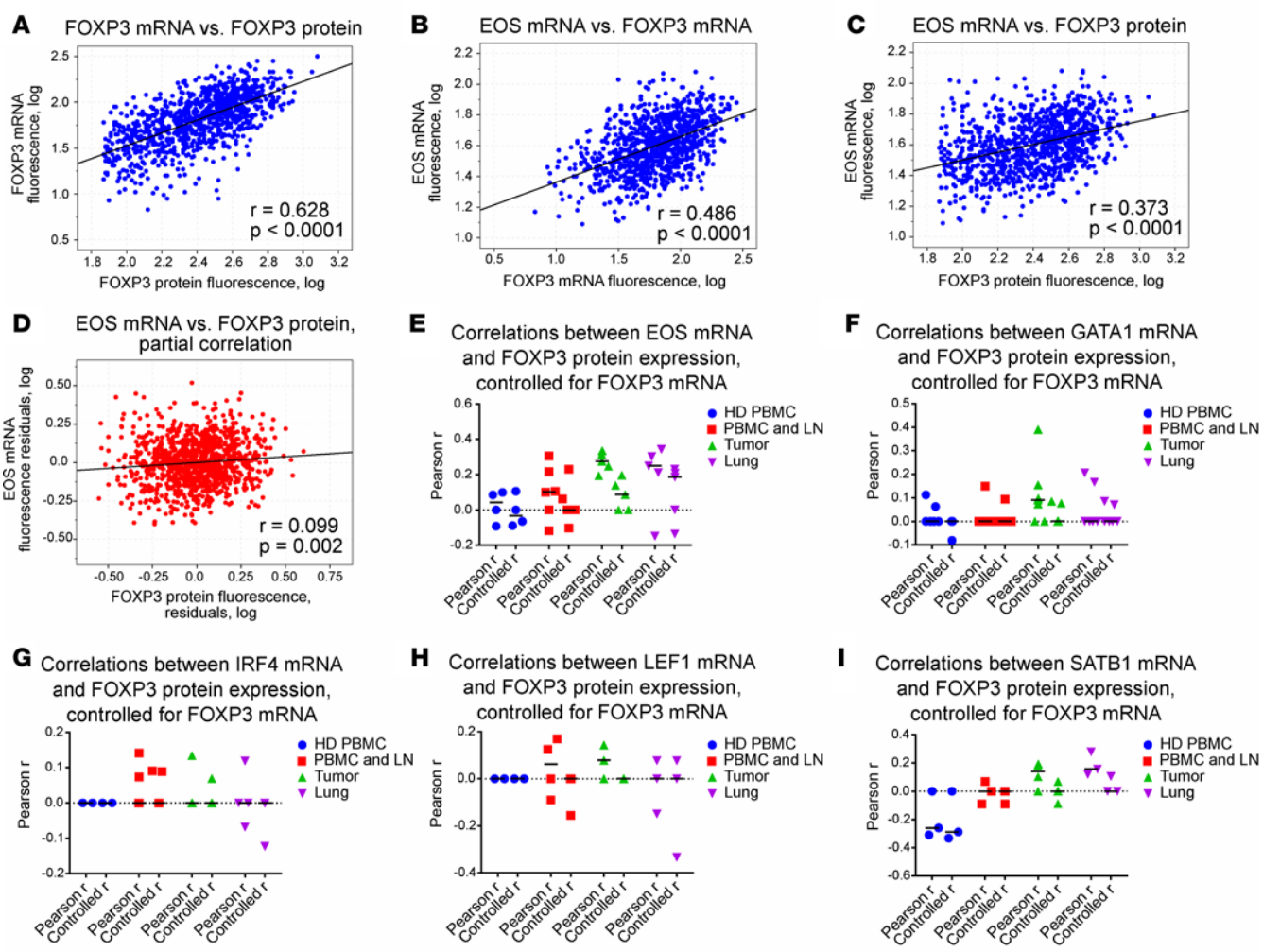

Figure 11. Correlations of Treg-locking TF expression and FOXP3 protein in Tregs. Data of fluorescence for markers of interest in CD4⁺FOXP3⁺ gated Tregs were collected using PrimeFlow method, exported as data for all channels in each individual Treg, log10 transformed, and evaluated for corresponding correlations. (**A–D**) An example of data obtained for one tumor sample. (**A**) FOXP3 mRNA correlates with FOXP3 protein expression on the single-cell level. EOS mRNA also correlates with (**B**) FOXP3 mRNA and with (**C**) FOXP3 protein expression in the same CD4⁺FOXP3⁺ Tregs, but (**D**) correlation between EOS mRNA and FOXP3 protein significantly decreased when controlled for FOXP3 mRNA. Those results correspond to 2 green triangles in **E**, with "Pearson *r*" = 0.373 and with partial correlation coefficient *r* ("Controlled *r*") = 0.099. (**E–I**) Results of partial correlation assays for 5 Treg-locking TFs, with every pair of symbols representing the assays illustrated in **A–D**. 1,000 Tregs (mean ± SEM) were evaluated in each sample, and each TF was evaluated at least twice (for healthy donors only) or 3 times, in different samples. The following statistics were used: (**A–D**) partial correlation assays and (**E–I**) Spearman correlation. When *P* values for any correlation were >0.05, then *r* presented as zeroes; detailed results are shown in Supplemental Table 6.

β-catenin (CTNNB1) (26), indoleamine-2,3-dioxygenase 1 (IDO1) (27), cyclooxygenase-2 (COX-2) (9, 28), and hypoxia-inducible factor-1α (HIF1a) (29, 30), a marker of hypoxia. β-Catenin and especially IDO1 tended to be upregulated in tumors in comparison with distant lung tissues, thereby providing potentially important pathways for future studies (Figure 12, G–L).

Discussion

Despite considerable clinical research indicating a generally negative prognostic relationship of Treg accumulation and growth of various tumors, there are very few studies analyzing the properties of FOXP3⁺ Tregs isolated from human tumors beyond their annotation and phenotyping by flow cytometry. The current study of Tregs isolated from patients with LC involves several innovations, including (a) the development and application of a method to deal with analysis of Tregs of varying purities in clinical isolates; (b) measurement of Treg function independent of other clinical variables; (c) an approach to quantitate iTreg versus tTreg numbers in clinical samples; and (d) application of the

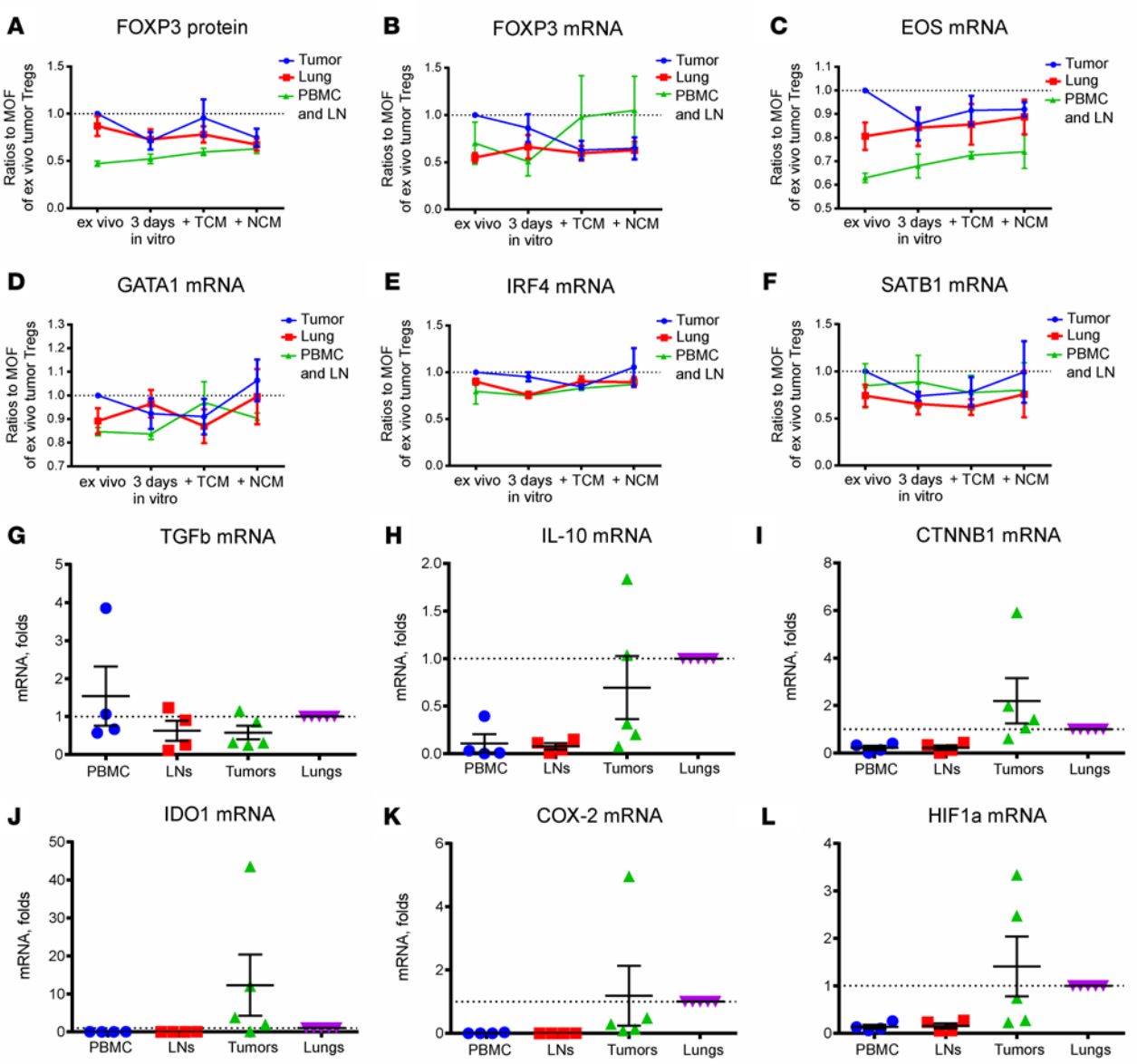

Figure 12. Stability of intratumoral Treg phenotype and tissue microenvironment. (**A–F**) mRNA of Treg-locking TFs in CD4$^+$FOXP3$^+$ Tregs were evaluated using PrimeFlow. Cell suspensions were incubated for 3 days in vitro in usual T cell media or 50% of volume was replaced by tumor-conditioned media (TCM) or distant lung-conditioned media (NCM). The expression of (**A**) FOXP3 protein, (**B**) FOXP3 mRNA, (**C**) EOS mRNA, (**D**) GATA1 mRNA, (**E**) IRF4 mRNA, and (**F**) SATB1 mRNA were evaluated in indicated samples, with expression of each marker in ex vivo tumor Tregs set as 1. Each marker was evaluated at least 2 times (in case of PBMCs and LNs) or at least 4 times (tumors and distant lungs). (**G–L**) RT-qPCR of single-cell suspensions of indicated samples for indicated markers. mRNA expression in lungs was set as 1, and at least 4 samples were evaluated for each mRNA.

PrimeFlow technique to analyze gene expression in 100% pure human Tregs. Using these assays, a series of insights were obtained.

From the outset, we did not find an increased population of Tregs in the blood of LC patients, in agreement with an observation that peripheral blood Treg numbers increase only during later cancer stages (1). However, when we studied patients preoperatively versus postoperatively, we noted that removal of tumors had negative effects on blood Treg numbers in patients with later stage and larger tumors, whereas stage IA patients had no changes in Treg or Teff numbers. Together, these data suggest that local events in lungs have little or no systemic effects on the immune system during the earliest stages of LC but start to affect blood Tregs as the tumors grow.

Some studies have previously reported increased numbers of intratumoral Tregs in LC patients using Treg numbers in peripheral blood as reference controls (31, 32). To our knowledge, only 2 prior studies evaluated

Treg numbers and phenotype in tumor tissues using adjacent lungs as controls (2, 33). Use of adjacent tumor-free tissue allows identification of tumor-specific, rather than tissue-specific, differences in Tregs and T cells, as discussed previously (34–36). In addition to showing increased numbers of Tregs in tumors compared with adjacent lung tissue, our study is the first to our knowledge to show tumor-specific increases in Treg numbers within lung LNs, even in early stages, when LNs are free of metastases. Increased LN Treg numbers were associated with decreased $CD8^+$ T cells within LC LNs, consistent with a recent observation that, in lung adenocarcinoma, Tregs restrict antitumor $CD8^+$ responses (2).

We explored various mechanisms to explain enrichment of Tregs in tumors, including expansion in situ, local iTreg conversion, and enhanced Treg recruitment (14). Our data did not support an enhanced division rate of intratumoral Tregs. Moreover, we found a negative correlation between $Ki67^+$ expression in Tregs and tumor size, suggesting that along with tumor growth, factors such as hypoxia, nutrient deprivation, and tumor necrosis may impair division of immune cells, including Tregs. A recent study of Tregs in human breast cancer came to a similar conclusion by showing that the TCR repertoires between normal tissue and tumor-associated Tregs did not overlap, suggesting that Tregs are recruited (36).

We next analyzed intratumoral iTreg conversion and found that none of our results supported this mechanism, consistent with earlier reports (36–38). We differentiated tTregs from iTregs using a previously developed method (19), which assesses a combination of FOXP3 expression, Treg-suppressive function, and methylation of the TSDR intronic site. Although iTregs and tTregs both share FOXP3 protein expression and suppressive function, only tTregs have a fully demethylated TSDR. In contrast, iTregs, which can be distinguished from activated human Teffs expressing FOXP3 by documenting suppressive function (39, 40), have only a partially demethylated TSDR (17, 18, 41). Thus, the ratio between FOXP3 protein expression and TSDR demethylation of the same Tregs that exhibit suppressive Treg function, is a measure allowing calculation of the percentages of iTregs and tTregs (19). If all $FOXP3^+$ cells are completely demethylated, i.e., if tTreg = 100%, then FOXP3/TSDR = 1. If there is a disruption of FOXP3 protein synthesis in completely TSDR-demethylated tTregs, e.g., in CNI-treated patients due to its negative effects on NFAT (42), then the FOXP3/TSDR is <1. In the current study, we showed that, in CNI-treated patients, the FOXP3/TSDR ratios were markedly decreased after transplant. Finally, if there are many $FOXP3^+$ cells that are partially demethylated, then FOXP3/TSDR is >1, similar to what we detected in pediatric transplant recipients treated with the mTOR inhibitor, rapamycin (19). In the current LC study, Tregs from all anatomic sites had the same FOXP3/TSDR ratios, arguing against intratumoral iTreg conversion. Surprisingly, those FOXP3/TSDR ratios were much higher than 1, corresponding to about 23% of iTregs (i.e., FOXP3/TSDR ratios were 1.3, which corresponds with $1:1.3 \approx 0.77$, i.e., 77% of tTregs, leading to $100\% - 77\% \approx 23\%$ iTregs). We hypothesized that the increased FOXP3/TSDR ratio might be explained by the advanced age of the patients and associated thymic involution. We found evidence to support this finding by comparing the youngest and oldest cohorts of pretransplant patients with lung disease. To our knowledge, this feature of increased iTreg population with age has been hypothesized for some years but has never been directly shown before.

To study Treg trafficking, we evaluated expression of 7 chemokine/chemokine receptors on Treg and Teffs. None were upregulated in tumor Tregs, but lung LN Tregs showed LC-specific upregulation of CXCR5. Given lack of upregulation of CXCL13, the only known ligand for CXCR5, the biological significance of this finding is unknown but may be related to the development of follicular helper subsets (20, 21) rather than Treg trafficking. Clearly our negative data may reflect Tregs trafficking to tumors via other chemokine/chemokine receptor interactions that were not tested here or that are not yet characterized. Our data also illustrate how studying adjacent nontumor lung tissue is a crucial control, as direct comparison of tumor Tregs to PBMC Tregs alone could have led to misleading findings. Alternatively, the increased numbers of intratumoral Tregs may be a result of another process, such as preferential survival of Tregs in tumor microenvironment and, therefore, their accumulation over time. This point is in agreement with our recent finding that FOXP3 reprograms T cells metabolism to survive in low glucose, high lactate environments (43). Overall, our data do not provide a biologic rationale for targeting of CCR4, CCR5, CCR7, CCR8, or CXCR3 to enhance antitumor immunity in LC patients.

Upon comparing the ability of tumor, lung, LN, and blood Tregs to suppress the proliferation of $CD4^+$ and $CD8^+$ HD responder T cells, we found that, while blood Tregs from LC patients were as suppressive as those from HD and those from patients listed for LT, intratumoral Tregs were distinguished by their more powerful suppressive capability. Our data correspond to findings in head and neck cancer (44) but not to others involving additional cancer types (8, 45, 46). In one study, intratumoral Tregs failed to suppress

proliferation of allogeneic blood T cells (8), whereas, in others, their suppressive function was not enhanced (45, 46). These discrepancies may be related to an absence of FOXP3$^+$ purity control of isolated Tregs and use of ^{3}H-thymidine incorporation as readout, as reviewed previously (22). Our study is the first to our knowledge to identify all isolated Tregs using FOXP3$^+$ cells, rather than CD4$^+$CD25$^+$ cells, after isolation and with adjustment of functional data according to differences in FOXP3$^+$ purity. As a result, to our knowledge, our study is the first involving functional tumor Treg data evaluated in a relatively large group of samples, with the best practices to ensure Treg phenotype.

To characterize the features of these potent intratumoral Tregs, we used distant lung tissue Tregs as controls to show that the observed phenotype was tumor specific rather than tissue specific. Most papers reporting tumor Treg-specific features involve comparison of tumor versus blood Tregs. However, tissue-resident Tregs and tumor Tregs have a largely shared phenotype that is quite different from peripheral blood Tregs (36). We also compared all Treg phenotypic data with corresponding CD4$^+$FOXP3$^-$ Teffs, as Treg-specific changes should not be mirrored by changes in the CD4$^+$FOXP3$^-$ subset. This approach, using two such control populations, to our knowledge, has never been used in Treg studies before. Our data showed that none of the 35 flow cytometry–based markers that were previously suggested to be Treg specific or even tumor Treg specific passed these restrictive criteria. Tim3 (47–49) was the best candidate to be termed tumor Treg-specific due to its high (although not unique) expression in intratumoral Tregs, although it did not reach statistically significant differences in tumor Tregs versus all other Tregs.

Finally, we applied the PrimeFlow assay to study RNA expression of FOXP3 and that of a quintet of TFs that were reported to help "lock" the transcriptional signature of Tregs in transduced murine T cells (13). In this study, enforced expression of FOXP3 with any one of the TFs, SATB1, EOS, LEF1, GATA1, or IRF4, led to robust induction of a Treg-specific gene signature, including upregulated and downregulated genes previously shown to be FOXP3 independent (13). We thus analyzed mRNA expression in 100% pure, i.e., CD4$^+$FOXP3$^+$, human Tregs versus CD4$^+$FOXP3$^-$ Teffs in all subsets (tumors, lungs, LNs, blood, and in HD) and found that tumor Tregs had a unique phenotype with significantly upregulated expression of 4 TFs, EOS, GATA1, SATB1, and IRF4, but not LEF1. Tumor Tregs also had twice as much FOXP3 mRNA per FOXP3$^+$ cell as any other Tregs and generated the highest correlation coefficients between FOXP3 mRNA and FOXP3 protein expressions. Single-cell analyses showed that mRNAs of all 5 TFs positively correlated with FOXP3 mRNA, with EOS and SATB1 in tumor Tregs having the highest correlation coefficients. In previous studies, EOS was shown to physically interact with FOXP3, repress FOXP3-regulated genes, and mediate Treg-suppressive function (50), and, of the 5 TFs studied, only EOS appeared to be involved in regulation of FOXP3 independent from FOXP3 mRNA, implying that it may be involved with posttranscriptional control of FOXP3, especially in tumor Tregs. However, this unique tumor Treg phenotype was not stable, since in vitro incubation led to significant loss of FOXP3 mRNA and protein and some decrease in the expression of Treg-locking TFs.

Although addition of tumoral soluble factors (TCM) did not prevent loss of FOXP3 and other TF mRNAs, it did rescue FOXP3 protein, suggesting that some as yet unknown soluble factors may regulate FOXP3 at the posttranslational level, e.g., as is known to occur by FOXP3 acetylation (51, 52). Peripheral Tregs, in turn, can be modified by exposure to soluble factors present in TCM. TCM-modified Tregs upregulated FOXP3 mRNA expression but failed to increase levels of all Treg-locking TFs (especially EOS) and did not increase FOXP3 protein to the levels comparable with ex vivo tumor Tregs. Together, our experiments indicate the importance of Treg-locking TFs in primary human Tregs, especially tumor Tregs. In agreement with earlier work (27), IDO may be the best candidate regulatory factor for Tregs in the LC microenvironment, since it showed the highest differences between tumors and all other samples, including distant lungs. Interestingly, IDO was previously shown to prevent loss of EOS in Tregs and therefore to block their reprogramming into T helper–like cells in inflammatory conditions in mice (53). This relationship as part of the tumor microenvironment will be studied in our future work. In addition, we plan to further investigate the factors controlling induction and high level expression of the Treg-locking TF quintet that our work indicates are linked with development of the hypersuppressive Tregs characteristic of human LC.

In conclusion, our study identifies distinctive features of intratumoral Tregs, and future immunotherapeutic strategies may require specific attention to the Treg-locking TF quintet as a means to decrease Treg function and promote antitumor therapy.

Methods

Patients and tissue samples. We studied 92 patients with LC, aged 68.0 ± 0.95 years old, 63% male, 73% with stage IA–IIA and 27% with stage IIB–IIIA (details are shown in Supplemental Table 7). We collected tumor, distant lung tissues, pulmonary LNs, and blood during the surgical resection of tumors, and, in 17 patients, we also collected blood at 3 months after tumor resection. HD PBMCs were obtained through the University of Pennsylvania Human Immunology Core, including a total of 23 donors, 17 male, with a mean age of 38.4 ± 2.3 years. Patients listed for LT served as an age-, sex-, and comorbidities-matched control group; they comprised 16 LT patients, aged 64.0 ± 2.0 years, 62.5% male (further details in the Supplemental Methods).

Cell isolation and culture. Surgically removed fresh lung tumors from patients were processed within 30 minutes of resection and digested with an enzymatic cocktail for 45–95 minutes with shaking, as described previously (54). We isolated PBMCs from blood using Ficoll-Paque Plus (GE Healthcare) gradient centrifugation, and we isolated LNs using mechanical dissection with a tissue grinder kit (Sigma-Aldrich). After isolation, cell numbers and viabilities were determined by trypan blue, and cells were rested overnight prior to the following studies. Cell culture media, TCM, and NCM are detailed in the Supplemental Methods.

Flow cytometry. Flow cytometry was performed with controls for cryopreservation, fixation, and permeabilization artifacts. We controlled antibody performance in groups of randomly picked sets of different patient samples with the same HD aliquots. Each of 35 cell markers was evaluated using at least 4 (for nonstimulated cells) or 3 (for GARP and LAP) different samples for each anatomical location. In total, we evaluated markers in 1,295 Treg-Teff pairs in 301 LC samples. We performed staining sequentially using fixable live/dead reagent, FC blocking, superficial antibodies staining, and fixation/permeabilization and intranuclear/intracellular antibody staining (details are in the Supplemental Methods).

PrimeFlow assay. We used the PrimeFlow RNA Assay (Affymetrix) according to the manufacturer's instructions, except for an incubation of cells with FOXP3 mAb for 1 hour instead of the recommended 30 minutes. A detailed list of reagents and procedures is provided in the Supplemental Methods.

TSDR FOXP3 methylation. This assay was performed as described previously (22) and as detailed in the Supplemental Methods. In brief, DNA isolated from Tregs was digested with 2 restriction enzymes, one methylation sensitive and the other methylation dependent. The next day, we amplified 4 products (no enzymes as "no digestion" control, both enzymes as "maximal digestion" control, and 2 products with each enzyme separately) with custom primers for human TSDR FOXP3 (EpiTect II DNA Methylation Enzyme Kit, Qiagen). CT qPCR data in triplicates were used to evaluate the percentage of demethylated and methylated TSDR, according to the manufacturer's instructions.

RT-qPCR. We isolated RNA with the RNeasy kit (Qiagen), synthesized cDNA (N8080234, ThermoFisher Scientific), and ran TaqMan gene expression assay with all primers from ThermoFisher Scientific.

Treg suppression assay. Briefly, $CD4^+CD25^+$ patient Tregs, isolated by magnetic beads (Miltenyi Biotec), were incubated with CFSE-labeled HD PBMCs at 1:1 to 1:16 Treg/PBMC ratios for 4 days. Cells were stimulated with CD3 mAb–coated microbeads at a ratio of 3.6 beads/cell. Aliquots of the same Tregs were cryopreserved just after isolation for $FOXP3^+$ purity control and for TSDR FOXP3 methylation assay. Suppressive function was counted as area under the curves, as described previously (19, 22). We used 3 LC (tumor) and 2 HD Tregs, gradually diluted with their own $CD4^+FOXP3^-$ Teffs (40%–100% Tregs in the mix) and tested them in suppression assays to determine how Tregs lose suppressive function with decreased $FOXP3^+$ purity after isolation (Figure 5D, Supplemental Figure 5B, and Supplemental Table 1). These data were used for regression analysis, and we applied the resulting equations (Supplemental Table 2) to adjust results of suppression assays according to exact $FOXP3^+$ purity of each isolated Treg sample.

iTreg conversion assay. We used $CD25^-$-depleted cells (130-091-301, Miltenyi-Biotec), controlled for very low and equal leftovers of $CD25^+FOXP3^+$ Tregs. Cells were stimulated for 7 days with CD3/28 beads (1:10), 10 ng/ml TGF-β, and 100 U/ml IL-2.

Statistics. All data were tested for normal distribution of variables, and then corresponding parametric (2-tailed Student's *t* test) or nonparametric tests were used, as detailed in the Supplemental Methods; *P* values of less than 0.05 were considered significant. Figures show mean ± SD.

Study approval. All studies were approved by the University of Pennsylvania Institutional Review Boards (811893, 813004, and 819345).

Author contributions

TA performed most of the experiments, evaluated data, performed statistical analyses, and wrote the manuscript. TZ, DN, and UHB performed flow cytometry. TZ also performed qPCR, PrimeFlow, cell isolation, and cell culture experiments and wrote the manuscript. EBE, SS, JS, AR, and MA performed LC tissue acquisition and processing. EBE also edited the manuscript, provided reagents, and acquired data. MHL, JMD, JDC, and UHB provided reagents, noncancer patient samples, and clinical data. WWH, SMA, TA, EBE, MHL, JMD, and JDC designed experiments and analyzed data. WWH, UHB, MHL, JS, and SMA edited the manuscript.

Acknowledgments

We thank Andrew Wheeler, University of Texas at Dallas, for his SPSS chart template file and corresponding guides. This work was supported in part by grants to WWH, "Treg Cells and Clinical Lung Cancer," from the Translational Center for Excellence of the University of Pennsylvania and from the NIH/National Cancer Institute (R01 CA177852). Other grant support included the Department of Defense (LC140199, W81XWH-15-1-0717 to EBE) and an NIH/National Cancer Institute grant (R01 CA187392-01A1 to EBE).

Address correspondence to: Wayne W. Hancock, Division of Transplant Immunology, Department of Pathology and Laboratory Medicine, Children's Hospital of Philadelphia, 3615 Civic Center Boulevard, Philadelphia, Pennsylvania 19104, USA. Phone: 215.590.8709; Email: whancock@mail.med.upenn.edu.

DN's present address is: Pathology Bioresource, Department of Pathology and Laboratory Medicine, University of Pennsylvania, Philadelphia, Pennsylvania, USA.

1. Erfani N, et al. Increase of regulatory T cells in metastatic stage and CTLA-4 over expression in lymphocytes of patients with non-small cell lung cancer (NSCLC). *Lung Cancer*. 2012;77(2):306–311.
2. Ganesan AP, et al. Tumor-infiltrating regulatory T cells inhibit endogenous cytotoxic T cell responses to lung adenocarcinoma. *J Immunol*. 2013;191(4):2009–2017.
3. Blanco JA, Toste IS, Alvarez RF, Cuadrado GR, Gonzalvez AM, Martín IJ. Age, comorbidity, treatment decision and prognosis in lung cancer. *Age Ageing*. 2008;37(6):715–718.
4. Marshall EA, et al. Emerging roles of T helper 17 and regulatory T cells in lung cancer progression and metastasis. *Mol Cancer*. 2016;15(1):67.
5. Tanaka A, Sakaguchi S. Regulatory T cells in cancer immunotherapy. *Cell Res*. 2017;27(1):109–118.
6. Petersen RP, et al. Tumor infiltrating Foxp3+ regulatory T-cells are associated with recurrence in pathologic stage I NSCLC patients. *Cancer*. 2006;107(12):2866–2872.
7. Domagala-Kulawik J, Osinska I, Hoser G. Mechanisms of immune response regulation in lung cancer. *Transl Lung Cancer Res*. 2014;3(1):15–22.
8. Woo EY, et al. Cutting edge: Regulatory T cells from lung cancer patients directly inhibit autologous T cell proliferation. *J Immunol*. 2002;168(9):4272–4276.
9. Shimizu K, Nakata M, Hirami Y, Yukawa T, Maeda A, Tanemoto K. Tumor-infiltrating Foxp3+ regulatory T cells are correlated with cyclooxygenase-2 expression and are associated with recurrence in resected non-small cell lung cancer. *J Thorac Oncol*. 2010;5(5):585–590.
10. Jackute J, et al. The prognostic influence of tumor infiltrating Foxp3(+)CD4(+), CD4(+) and CD8(+) T cells in resected non-small cell lung cancer. *J Inflamm (Lond)*. 2015;12:63.
11. Droeser R, et al. Differential pattern and prognostic significance of CD4+, FOXP3+ and IL-17+ tumor infiltrating lymphocytes in ductal and lobular breast cancers. *BMC Cancer*. 2012;12:134.
12. Ladoire S, Martin F, Ghiringhelli F. Prognostic role of FOXP3+ regulatory T cells infiltrating human carcinomas: the paradox of colorectal cancer. *Cancer Immunol Immunother*. 2011;60(7):909–918.
13. Fu W, et al. A multiply redundant genetic switch 'locks in' the transcriptional signature of regulatory T cells. *Nat Immunol*. 2012;13(10):972–980.
14. Ondondo B, Jones E, Godkin A, Gallimore A. Home sweet home: the tumor microenvironment as a haven for regulatory T cells. *Front Immunol*. 2013;4:197.
15. Hanahan D, Weinberg RA. Hallmarks of cancer: the next generation. *Cell*. 2011;144(5):646–674.
16. Abbas AK, et al. Regulatory T cells: recommendations to simplify the nomenclature. *Nat Immunol*. 2013;14(4):307–308.
17. Baron U, et al. DNA demethylation in the human FOXP3 locus discriminates regulatory T cells from activated FOXP3(+) conventional T cells. *Eur J Immunol*. 2007;37(9):2378–2389.
18. Floess S, et al. Epigenetic control of the foxp3 locus in regulatory T cells. *PLoS Biol*. 2007;5(2):e38.
19. Akimova T, et al. Differing effects of rapamycin or calcineurin inhibitor on T-regulatory cells in pediatric liver and kidney transplant recipients. *Am J Transplant*. 2012;12(12):3449–3461.
20. Linterman MA, et al. Foxp3+ follicular regulatory T cells control the germinal center response. *Nat Med*. 2011;17(8):975–982.

21. Chung Y, et al. Follicular regulatory T cells expressing Foxp3 and Bcl-6 suppress germinal center reactions. *Nat Med*. 2011;17(8):983–988.
22. Akimova T, Levine MH, Beier UH, Hancock WW. Standardization, evaluation, and area-under-curve analysis of human and murine Treg suppressive function. *Methods Mol Biol*. 2016;1371:43–78.
23. Henning AL, Sampson JN, McFarlin BK. Measurement of low-abundance intracellular mRNA using amplified FISH staining and image-based flow cytometry. *Curr Protoc Cytom*. 2016;76:7.46.1–7.46.8.
24. Pickup M, Novitskiy S, Moses HL. The roles of TGFβ in the tumour microenvironment. *Nat Rev Cancer*. 2013;13(11):788–799.
25. Jeon HS, Jen J. TGF-beta signaling and the role of inhibitory Smads in non-small cell lung cancer. *J Thorac Oncol*. 2010;5(4):417–419.
26. Stewart DJ. Wnt signaling pathway in non-small cell lung cancer. *J Natl Cancer Inst*. 2014;106(1):djt356.
27. Munn DH, Mellor AL. IDO in the tumor microenvironment: inflammation, counter-regulation, and tolerance. *Trends Immunol*. 2016;37(3):193–207.
28. Sandler AB, Dubinett SM. COX-2 inhibition and lung cancer. *Semin Oncol*. 2004;31(2 Suppl 7):45–52.
29. Ren W, et al. The expression of hypoxia-inducible factor-1α and its clinical significance in lung cancer: a systematic review and meta-analysis. *Swiss Med Wkly*. 2013;143:w13855.
30. Kumar V, Gabrilovich DI. Hypoxia-inducible factors in regulation of immune responses in tumour microenvironment. *Immunology*. 2014;143(4):512–519.
31. Shigematsu Y, et al. Immunosuppressive effect of regulatory T lymphocytes in lung cancer, with special reference to their effects on the induction of autologous tumor-specific cytotoxic T lymphocytes. *Oncol Lett*. 2012;4(4):625–630.
32. Woo EY, et al. Regulatory CD4(+)CD25(+) T cells in tumors from patients with early-stage non-small cell lung cancer and late-stage ovarian cancer. *Cancer Res*. 2001;61(12):4766–4772.
33. Schneider T, et al. Foxp3(+) regulatory T cells and natural killer cells distinctly infiltrate primary tumors and draining lymph nodes in pulmonary adenocarcinoma. *J Thorac Oncol*. 2011;6(3):432–438.
34. Thome JJ, Farber DL. Emerging concepts in tissue-resident T cells: lessons from humans. *Trends Immunol*. 2015;36(7):428–435.
35. Turner DL, et al. Lung niches for the generation and maintenance of tissue-resident memory T cells. *Mucosal Immunol*. 2014;7(3):501–510.
36. Plitas G, et al. Regulatory T cells exhibit distinct features in human breast cancer. *Immunity*. 2016;45(5):1122–1134.
37. Wang C, Lee JH, Kim CH. Optimal population of FoxP3+ T cells in tumors requires an antigen priming-dependent trafficking receptor switch. *PLoS One*. 2012;7(1):e30793.
38. Hindley JP, et al. Analysis of the T-cell receptor repertoires of tumor-infiltrating conventional and regulatory T cells reveals no evidence for conversion in carcinogen-induced tumors. *Cancer Res*. 2011;71(3):736–746.
39. Wang J, Ioan-Facsinay A, van der Voort EI, Huizinga TW, Toes RE. Transient expression of FOXP3 in human activated non-regulatory CD4+ T cells. *Eur J Immunol*. 2007;37(1):129–138.
40. Tran DQ, Ramsey H, Shevach EM. Induction of FOXP3 expression in naive human CD4+FOXP3 T cells by T-cell receptor stimulation is transforming growth factor-beta dependent but does not confer a regulatory phenotype. *Blood*. 2007;110(8):2983–2990.
41. Polansky JK, et al. DNA methylation controls Foxp3 gene expression. *Eur J Immunol*. 2008;38(6):1654–1663.
42. Tang Q, Bluestone JA, Kang SM. CD4(+)Foxp3(+) regulatory T cell therapy in transplantation. *J Mol Cell Biol*. 2012;4(1):11–21.
43. Angelin A, et al. Foxp3 reprograms T cell metabolism to function in low-glucose, high-lactate environments. *Cell Metab*. 2017;25(6):1282–1293.e7.
44. Strauss L, Bergmann C, Szczepanski M, Gooding W, Johnson JT, Whiteside TL. A unique subset of CD4+CD25highFoxp3+ T cells secreting interleukin-10 and transforming growth factor-beta1 mediates suppression in the tumor microenvironment. *Clin Cancer Res*. 2007;13(15 Pt 1):4345–4354.
45. Wolf AM, Wolf D, Steurer M, Gastl G, Gunsilius E, Grubeck-Loebenstein B. Increase of regulatory T cells in the peripheral blood of cancer patients. *Clin Cancer Res*. 2003;9(2):606–612.
46. Liyanage UK, et al. Prevalence of regulatory T cells is increased in peripheral blood and tumor microenvironment of patients with pancreas or breast adenocarcinoma. *J Immunol*. 2002;169(5):2756–2761.
47. Anderson AC. Tim-3: an emerging target in the cancer immunotherapy landscape. *Cancer Immunol Res*. 2014;2(5):393–398.
48. Bu M, et al. Ovarian carcinoma-infiltrating regulatory T cells were more potent suppressors of CD8(+) T cell inflammation than their peripheral counterparts, a function dependent on TIM3 expression. *Tumour Biol*. 2016;37(3):3949–3956.
49. Gao X, et al. TIM-3 expression characterizes regulatory T cells in tumor tissues and is associated with lung cancer progression. *PLoS One*. 2012;7(2):e30676.
50. Pan F, et al. Eos mediates Foxp3-dependent gene silencing in CD4+ regulatory T cells. *Science*. 2009;325(5944):1142–1146.
51. Liu Y, et al. Inhibition of p300 impairs Foxp3$^+$ T regulatory cell function and promotes antitumor immunity. *Nat Med*. 2013;19(9):1173–1177.
52. van Loosdregt J, et al. Regulation of Treg functionality by acetylation-mediated Foxp3 protein stabilization. *Blood*. 2010;115(5):965–974.
53. Sharma MD, et al. An inherently bifunctional subset of Foxp3+ T helper cells is controlled by the transcription factor eos. *Immunity*. 2013;38(5):998–1012.
54. Quatromoni JG, Singhal S, Bhojnagarwala P, Hancock WW, Albelda SM, Eruslanov E. An optimized disaggregation method for human lung tumors that preserves the phenotype and function of the immune cells. *J Leukoc Biol*. 2015;97(1):201–209.